STABLE ORGANIC ISOTOPIC ($\delta^{15}N_{ORG}$, $\delta^{13}C_{ORG}$) EVIDENCE FOR CLIMATE-FORCED LANDSCAPE AND AQUATIC CHANGE DURING THE LATE HOLOCENE IN ABACO ISLAND, THE BAHAMAS

A Thesis

by

ANNE ELIZABETH TAMALAVAGE

Submitted to the Office of Graduate and Professional Studies of
Texas A&M University
in partial fulfillment of the requirements for the degree of

MASTER OF SCIENCE

Chair of Committee,	Patrick Louchouarn
Co-Chair of Committee	Peter van Hengstum
Committee Members,	Karl Kaiser
	Deborah Thomas
	Eric Riggs
Head of Department,	Deborah Thomas

August 2016

Major Subject: Oceanography

ABSTRACT

The sediments that have accumulated in Blackwood Sinkhole preserve a 3000-year record of environmental change on Abaco Island, Northern Bahamas. Previous palynological data reveal that Abaco's forest structure has not been constant during the late Holocene (last 3000 years), likely in response to local precipitation changes from southern migration of the Intertropical Convergence Zone (ITCZ) at 1000 Cal yrs BP. This thesis investigates the geochemical record of forest structure change with geochemical signals ($\delta^{13}C_{org}$ and $\delta^{15}N_{org}$, C:N and Lignin-derived CuO Oxidation Products (LOP)) preserved by the bulk sedimentary organic matter (OM) within Blackwood Sinkhole.

Currently, the northern Bahamian islands (Abaco, Andros, Grand Bahamas, and New Providence) receive greater annual precipitation than those further to the south, which may be generating sufficiently mesic conditions for the northern islands to support *Pinus* forests. Geochemical proxies reveal shifts in OM sources throughout the core that can be classified under three distinct groupings. Measured variation in the geochemical proxies remains consistent with the effects of a southern displacement of the ITCZ at 1000 Cal yrs BP. Group 3 (approximately, 1500-3000 YBP (1700 YBP in core 3)) is characterized by a depleted $\delta^{13}C_{org}$ signature (relative to group 1), a higher mean S/V ratio relative to group 1, the highest mean C:N ratio, and a dominance of *Myrtaraceae* and *Arecaceae*. Group 2 (approximately 1000-1500 YBP) is defined by a higher mean $\delta^{15}N_{org}$ signature, the most depleted $\delta^{13}C_{org}$ signature, an increase in soft tissue LOP signatures (Cinnamyl/Vanillyl, C/V ratio), and a presence of *Lemna* spores

within the interval. Group 1 (approximately 0-1000 YBP) is predominantly defined by a relatively enriched $\delta^{13}C_{org}$ signature, a lower Syringyl/Vanillyl (S/V) LOP ratio, and an emergence of *Conocarpus, Pinus*, and *Typha angustifolia.* OM source changes, defined by the measure of $\delta^{13}C_{org}$ and $\delta^{15}N_{org}$, C:N and LOP signatures, within Blackwood Sinkhole support the previously compiled palynological reconstruction of forest structure change, and record regional terrestrial and aquatic response (of the surrounding watershed and in the sinkhole) to larger scale climatic changes through time.

DEDICATION

I would like to dedicate this thesis in memory of John J. Tamalavage. Without his constant support (both financial and emotional), and encouragement (albeit sometimes with some pushback) to pursue every opportunity that could refine and progress my skill set, I would have never been able to write this document. Thank you immensely, Dad.

ACKNOWLEDGEMENTS

I would like to send an enormous thanks to my committee chairs, Dr. Patrick Louchouarn and Dr. Pete van Hengstum, for giving me a chance to pursue this research, for their continuous advice and guidance, and for their trust in my ability to explore and answer geochemical questions. Thank you to my committee members, Dr. Deborah Thomas, Dr. Eric Riggs, and Dr. Karl Kaiser for their support and input not only to my professional development within my Master's (and future career), but also analytical expertise.

A special thanks goes to Dr. Patricia L. Fall for her compiled palynological record and analysis. Additionally, I would like to thank Dr. Jeffrey P. Donnelly for his collaboration within this project. Thank you to my friends and colleagues and the department faculty and staff (of both the MARS and OCNG departments) for making my time at Texas A&M University a great experience. My thanks includes but is not limited to the expertise and support given by Matt Norwood, Amanda Sterne, Nikki West, Kendra Kopp, Shawna Little, Richard Sullivan, Tyler Winkler, Tori Keeton, Gary Maale, Jake Emmert, Jacque Cresswell, Maria Canedo, Danielle Creely, Alexandra Rivard, Kevin Warner, Matt Athon, David Brankovits, Claire McKinley, and Noura Randle. I would also to particularly like to thank Sergey Molodstov, who helped me immensely with the Python code, Allison Myers-Pigg for her analytical expertise and advice, and Andrew McGuffin for his unyielding support and encouragement. I would additionally and importantly like to thank my mother, Rita Tamalavage, for her openness with communication, and her support and love.

NOMENCLATURE

OM	Organic Matter
BLWD	Blackwood
C2/C3/C6	Core 2, Core 3, Core 6
ITCZ	Intertropical Convergence Zone
OC	Organic Carbon (%)
C:N	Carbon to Nitrogen atomic ratio
Cal yrs BP	Calibrated years Before Present
DIN	Dissolved Inorganic Nitrogen
TC	Total Carbon (%)
TN	Total Nitrogen (%)
LOP	Lignin-dervide CuO Products

TABLE OF CONTENTS

Page

LIST OF FIGURES

Page

LIST OF TABLES

Page

1. INTRODUCTION

ITCZ migrations are impacted by sea surface temperature gradients and larger changes in overturning circulations, influencing precipitation variability throughout the North Atlantic (Chiang, 2002; Jury et al., 2007; Waliser and Gautier, 1993). Spatial variability within the Caribbean supports regional inconsistencies in precipitation, due to larger climatic shifts (e.g., Jury et al., 2007; Gamble and Curtis, 2008). Variability in precipitation within regions affected by the ITCZ can impact regional vegetation and hydrology, recorded in sedimentary organic matter (e.g., Kjellmark, 1996; Lee-Thorp et al. 2001; Lane et al. 2014).

Sedimentary changes recorded within Blackwood Sinkhole on Abaco Island in the northern Bahamas suggest that meridional migration of the Intertropical Convergence Zone (ITZC) over the late Holocene has modulated intense hurricane landfalls on the western North Atlantic margin. (van Hengstum et al., 2016). Previously compiled palynological records from Abaco island suggest that forest structure has not remained constant over the late Holocene (last 3000 years) (Slayton, 2010; van Hengstum et al., 2016). Currently, the northern Bahamian islands (Abaco, Andros, Grand Bahamas, and New Providence) receive greater annual precipitation than those further to the south, which may be generating sufficiently mesic conditions for the northern islands to support *Pinus* forests (Jury et al., 2007; van Hengstum et al. 2016). Geochemical markers ($\delta^{13}C_{org}$ and $\delta^{15}N_{org}$ signatures, atomic C:N ratio, and lignin-derived CuO Oxidation Products (LOP)) extracted from the sedimentary record can test the hypothesis that a migration in the position of the ITCZ at 1000 calibrated years before

present (Cal yrs BP) impacted a significant change in rainfall, causing changes in regional terrestrial vegetation and hydrology.

These thesis attempts to provide a reconstruction of ecological change throughout the late Holocene on Abaco island using geochemical markers. The extraction and quantification of these proxies were motivated by the following questions: 1) Do stable isotopic signatures ($\delta^{13}C_{org}$ and $\delta^{15}N_{org}$) and elemental ratio (atomic C:N) of bulk organic matter deposited into Blackwood Sinkhole document regional landscape (e.g., forest structure) changes and/or changes to aquatic productivity in the sinkhole basin itself? 2) Do lignin-derived CuO oxidation products (LOP) within the sedimentary bulk organic matter (OM) provide evidence for the predominance of angiosperm (e.g., palms, myrtles) versus gymnosperm (pines) plants on the landscape?

2. LITERATURE REVIEW

2.1 Caribbean Climate

The ITCZ is a narrow, tropical (centered around 6°N of the equator) belt of deep convective clouds that migrates between 9°N and 2°N in boreal winter over the central Atlantic and Pacific oceans. It can be classified as the feature (within the tropics) that most vividly displays the meeting of the two hemispheres (Waliser and Gautier, 1993; Chiang et al., 2002; Schneider et al., 2014). The ITZC is fed by the trade winds that are full with heat and moisture, that converge to form a zone of convection, cloudiness and precipitation (Waliser and Gautier, 1993; Schneider et al., 2014). The ITCZ cycles within the equatorial trough and makes up the ascending branch of the Hadley circulation (Waliser and Gautier, 1993). Simulations and observed dynamics of the ITCZ indicate that it migrates meridionally (impacted by changes in overturning circulations, and Atlantic sea surface temperature (SST) gradients) and its rainfall intensity changes when the atmospheric energy balance shifts (due to convective release of latent heat) (Waliser and Gautier, 1993; Chiang et al., 2002; Schneider et al., 2014). Understanding the position, structure, and migration of the ITCZ can help define global climate changes, and air-sea interactions at a regional scale (Waliser and Gautier, 1993).

Understanding precipitation variability within the Caribbean remains complex. Groupings (four, spanning the entirety of the Caribbean islands between Florida and Venezuela) within the Caribbean have shown distinct precipitation regions, based on changes of annual cycles and residual fluctuations within each grouping (Jury et al., 2007). Additionally, a five-part (North Atlantic high pressure, low level Caribbean jet,

subsidence caused by Central America convection, basin wide increased wind shear, and divergence around Jamaica) regional precipitation model addresses spatial variability within annual rainfall and drought throughout the Caribbean (Gamble and Curtis, 2008).

Within regions affected by fluctuations and dynamics of the ITCZ, recordings of Late Holocene climatic changes (associated with such migrations of the ITCZ) have been measured using various geochemical proxies. Lee-Thorp et al. (2001) measured stable carbon and oxygen isotopes on a stalagmite in Cold Air Cave, Makapagnsgat Valley, southeastern Africa to discover that there was a fundamental transition from humid and warm conditions to drier and cooler, lasting 3200 to 1750 Cal yrs BP. Haug et al. (2003) measured bulk sediment Titanium (%) from riverine inputs into the anoxic Cariaco basin to find that an extended period of drought impacted the southern Caribbean during the last 2000 years. From measuring stable oxygen isotopes from stalagmite records in Cuba, Fensterer et al., (2012, 2013) records that a southern position of the ITCZ results in drier conditions in Cuba throughout the late Holocene, but also suggests an increase in precipitation at 1000 Cal yrs BP. These records correlate (on millennial timescales) to SST variability from West Africa, suggesting the large-scale connection of ITCZ migrations impact temperature and precipitation variability (Fensterer, 2013).

Compiled by Schneider et al. (2014), time periods that include a higher Northern-to-Southern interhemispheric temperature anomaly, increased rainfall (measured through $\delta^{18}O$), and higher weight percent of elemental titanium, correlate to a more Northern position of the ITCZ (meaning a wetter time period) throughout the last

12,000 years. At 1000 cal. years BP, there is an abrupt shift within the interhemispheric temperature anomaly (more negative) that informs a southern migration of the ITCZ (Schneider et al., 2014).

Caribbean terrestrial landscape reconstructions (e.g., pollen, precipitation) also indicate considerable variability during the late Holocene, which have also been linked to merdional ITCZ variability (e.g., Kjellmark, 1996). Through palynological analysis, Kjellmark (1996) suggests that there was a dry period on Andros island from 3200 to 1500 Cal yrs BP in which dry, shrubland vegetation dominated. A more mesic (humid) climate supported tropical hardwoods and an eventual emergence of pines (approximately 1500 Cal yrs BP). Late Holocene terrestrial vegetation and limnological changes have additionally shown relationships with precipitation variability associated with millennial-scale migrations of the ITCZ within the Caribbean (e.g., Lane et al., 2014). Lane et al. (2014) utilized geochemical proxies, specifically terrestrial-derived leaf waxes (*n*-alkanes), from sedimentary horizons (lacustrine cores from the Dominican Republic) and measured compound specific Deuterium/Protium (D/H) ratios to infer precipitation trends through time (specifically through the terminal classic drought). This work reveals that vegetation (even if potentially influenced anthropogenically through advances in agriculture) does not remain constant in the late Holocene in the Caribbean.

2.2 Sinkhole Basins

Caves, cenotes, blueholes and sinkholes are common features within karst basins (van Hengstum et al., 2011). Karst basins are globally distributed and provide a

record of climatic variability during the late Holocene (e.g., Kjellmark, 1996; Kovacs et al., 2013; Fensterer et al., 2013; van Hengstum et al., 2016). Sinkholes are water-filled vertical openings in carbonate rock that can develop from the long-term dissolution of limestone bedrock, and are created by a mechanism that can produce a deep, flooded void that is open to the surface (Mylorie et al., 1995).

Porosity of karst allows for the uninhibited circulation of groundwater through karst basins (van Hengstum et al., 2011). Karst basins can be defined as saturated, or unsaturated relative to the amount and positioning of underlying groundwater and meteoric influence (Mylroie et al., 1999). The porosity of the limestone bedrock promotes tidal exchange with the aquifer, with volume and fluxes influenced by porosity, proximity to the coast, and permeability depending on the carbonate platform (Martin et al., 2012). Sinkholes are typically characterized by stratification between hydrographic layers (an upper, freshwater lens, a mixing zone, and a lower layer of saline groundwater) (Mylorie et al., 1995). Tidal pumping can affect conductivity of water within coastal sinkholes and blue holes and additionally influence dissolution rates and patterns (Martin et al., 2012). Regional geomorphologic and hydrologic changes can impact groundwater flow and hydrologic stratification within sinkholes, allowing for a turbulent interaction with saline groundwater and the upper fresh, meteoric lens (van Hengstum et al., 2010). The karst geology, hydrographic variability and proximity to the coastline create a unique environment within sinkholes that promotes complex ecologies and water chemistries, informing changes within karst processes, global climate, marine ecology and geochemistry (Mylroie et al., 1995).

2.3 Stable Isotopes ($\delta^{13}C_{org}$ and $\delta^{15}N_{org}$) and C:N Ratio

Geochemical proxies such as $\delta^{13}C_{org}$ and $\delta^{15}N_{org}$ signatures, Organic Carbon (OC), Total Nitrogen (TN), and C:N ratio can be used to trace particular plant sources contributing to organic matter provenance within coastal environments (Peters et al., 1978; Hedges et al. 1997; Lamb et al., 2006). Holocene sediments have been analyzed for such geochemical proxies as an indicator of coastal environments relative to sea level (Lamb et al., 2006).

Variations in $\delta^{13}C_{org}$ signatures are due to photosynthetic plants utilizing different photosynthetic pathways (O'Leary, 1981). Most terrestrial plants utilize the C_3 pathway and have an average $\delta^{13}C_{org}$ value of −28‰ (O'Leary, 1988; Lamb et al., 2006). C_4 plants display changes in CO_2 fixation, influenced by the PEP enzyme (carboxylation of phosphoenolpyruvate) and have typical $\delta^{13}C_{org}$ values of −14‰ (O'Leary, 1988; Lamb et al., 2006). Additionally, some plants (like succulents) can incorporate both C_3 and C_4 pathways and are categorized as CAM (crassulacean acid metabolism) plants. CAM plants can display $\delta^{13}C_{org}$ values ranging from −27 to −13‰ (variation in isotopic signatures of CAM plants is influenced very strongly by temperature and light availability), (O'Leary, 1981; Lamb et al., 2006). Marine-derived organic matter, and freshwater aquatic plants can range from −22 to −20‰ and −50 to −11‰, respectively (Meyers, 1994; Keeley and Sandquist, 1992; Lamb et al., 2006).

Nitrogen isotopic signals are useful tool for paleo-environmental reconstruction and determining the provenence of OM for both terrestrial and aquatic plants. During assimilation photosynthetic plants fractionate inorganic nitrogen sources (NH_4, N_2, NO_2,

NO_3) (Fogel and Cifuentes, 1993; Talbot and Laerdal, 2000). Within terrestial plants, soil bacteria influence nitrogen sources utilized during assimilation, and such source changes can be reflected in isotopic signatures (Peters et al., 1978; Talbot and Laederal, 2000). Within the aquatic system, $\delta^{15}N_{org}$ signatures of phytoplankton and algae are influenced strongly by DIN source composition (Peters et al., 1978). $\delta^{15}N_{org}$ signatures can be used to understand allochthonous organic matter versus autochthonous plankton debris within a lacustrine system (Duck, 1986). Aquatic algae preferentially discriminate against ^{15}N during assimilation, resulting in lighter $\delta^{15}N_{org}$ signatures than the DIN pool. With increased productivity (resulting in phytoplankton blooms), $\delta^{15}N_{org}$ signatures could be higher because of the DIN pool becoming progressively enriched in ^{15}N (Talbot and Laerdal, 2000; Brandenberger et al., 2011). Additionally, $\delta^{15}N_{org}$ signatures can help to differentiate marine versus terrestrial sources (Peters et al., 1978; Brandenberger et al., 2011). To deconstruct marine and terrestrial contributions in a coastal system, end-member values of 7-9‰(average, ~8‰) and 1-4‰ (average ~3‰) for marine and terrestrial OM (respectively) are accepted (Fogel and Cifuentes, 1993; Brandenberger et al., 2011).

Understanding changes within the $\delta^{15}N$ of particulate nitrogen, relative to $\delta^{15}N$ of DIN can help to trace algal productive (from regenerated nitrogen), nitrogen fixation, dentrificiation, and changes in trophic structure (Fogel and Cifuentes, 1993). The assimilation and contributions of nitrogen to OM within the system can reflect OM source, but $\delta^{15}N$ signatures could also could be influenced by additional biogeochemical processes or alteration.

$\delta^{13}C_{org}$ values remain a strong indicator of OM source, and when combined with $\delta^{15}N_{org}$ signatures, isotopic changes can provide thorough analyses of source type or biogeochemical processes within the water column. Particularly, stable isotope mixing models are useful for quantifying source contributions to a mixture (Phillips et al., 2005). Models require reliable endmembers to categorize source-types that can be contributing within the system. Fraction of contributions to the OM (such as terrestrial, marine, allochthonous, and authothonous) can be determined.

C:N additionally remains an important ratio to deconstruct original source and plant type (yet, it can be sensitive to decomposition during preservation (Wilson et al., 2005)). Terrestrial vegetation records high C:N ratios, 12 to 14 (Prahl et al., 1980), because it is dominated by nitrogen-poor lignin and cellulose (Lamb et al., 2006). Unaltered marine OM typically records C:N ratios of 4 to 7(Prahl et al., 1980).

Carbon and nitrogen isotopic signatures (and C:N ratio) measured from sedimentary have remained useful in understanding OM source reconstructions on Holocene timescales (e.g., Lamb et al., 2006; Filley et al., 2001; van Hengstum et al., 2010; Gouveia et al., 2002; Talbot & Laerdal, 2000). However, some depositional environments, such as mangrove systems, remain difficult to constrain. Within mangrove systems, $\delta^{13}C_{org}$ signatures can be utilized to track source contributions (which can include seagrasses, mangrove vegetation and phytoplankton), while $\delta^{15}N_{org}$ signatures can help to understand biochemical changes of OM with burial (Gonneea et al., 2004). However, uneven sedimentation rates, confounding relationships between

changes in salinity and carbon isotopic signatures can impact their utility in OM source reconstructions (Ladd and Sachs, 2015)).

2.4 Lignin

Bulk organic signatures are successful in understanding heterogeneity and changing sources of terrigenous OM in paleoclimatic reconstructions. (Louchouarn et al., 2006; Meyers et al., 1999; Goni, 1997). However, bulk signatures are limited in reconstructing specific plant-type contributions within an environmental system. When understanding specific or advanced information about a system for reconstruction, the bulk OM signal represents a combination of fractions of plants/algae that utilize different biosynthetic pathways, and may not be best for quantifying specific vegetation types or processes (Sachse et al., 2012).

Specifically, the high chemical stability of the phenolic polymers that characterize lignin compounds (and the fact that these compounds are absent from all other living organisms, except for vascular plants), make them an effective organic geochemical tracer (Hedges and Mann, 1979). Two main groupings of plants can be defined clearly by biochemical compositions. Non-vascular plants contain little or no lignin (e.g., phytoplankton) and vascular plants are characterized by high concentrations of cellulose and lignin (e.g., shrubs, grasses, and trees) (Meyers and Verges, 1999). There are exceptions to these groupings (e.g., bryophytes contain cellulose, but no lignin).

Within the lignin macromolecule, 11 phenols (divided into four different structural families) contribute to plant tissues sources within a sample (either plant or sediment) (Hedges and Ertel, 1982). Specifically, p-hydroxyl, vanillyl and syringyl have three

phenols each (aldehyde, ketone, and carboxylic acid). Cinnamyls have two phenols (Hedges and Ertel, 1982). The lignin macromolecule is large and remains difficult to quantify. Through chemical alteration (oxidation and extraction), specific phenols can be isolated and preserve the characteristics of the original polymers (Hedges and Ertel, 1982).

Lignin can be a useful tool in paleo-vegetation reconstructions of coastal environments because of the specificity that exists between the relationship of lignin phenols and plant-type (typically angiosperms versus gymnosperms), and that lignin molecules are resistant to diagenesis within marine sediments (Hedges and Ertel, 1982; Hedges and Parker, 1976; Hedges and Mann, 1979; Visser et al., 2004). Ratios of the vanillyl (V), syringyl (S) and cinnamyl (C) phenols, described as S/V, C/V extracted from sediments, can be used to differentiate sources of terrestrial organic matter (Hedges and Mann, 1979; Visser et al., 2004). Woody and non-woody tissues of both angiosperms and gymnosperms yield different combinations of phenols (Hedges and Ertel, 1982). For example, LOP were analyzed in Holocene sediments from a sinkhole lake in Florida, which isolated regional vegetation changes that was also detected in the $\delta^{13}C_{org}$ ratios of bulk sediment (Filley et al., 2001).

Common data reporting includes a measurement of $\Lambda 8$, which is the sum of the three major lignin components (syringyls, vanillyls, and cinnanmyls), normalized to 100 mg OC in the sample, and this value remains useful for quantifying both estuarine sediments and fresh plant fractions (Hedges and Ertel, 1982; Goñi and Thomas, 2000; Houel et al., 2006). Selected transport and physical influences (e.g., discharge, dispersal,

biogeochemical cycling) affecting organic matter deposition into marine systems can also be constrained through using lignin biomarkers (Louchouarn et al., 1997,1999; Farella et al., 2001; Bianchi et al., 2002; Feng et al., 2015). Ratios of the lignin-derived CuO oxidation products can also reconstruct the extent of degradation of the lignin macromolecule within sediments (Goñi et al., 2000;Visser et al., 2004; Houel et al., 2006). Specifically, Acid/Aldehyde (typically reported relative to the vanillyls because they constitute more than 80% of all lignin products (Goñi et al., 2000).

3. STUDY SITE

The Bahamas are characterized by a group of carbonate (carbonate sourced from both biogenic and authigenic processes) islands and banks covering 300,000 km^2 in the North Atlantic Ocean (Carew and Mylorie, 1997). Geologically, the islands are typically low-lying and preferentially occur on the eastern side of the banks (build up of such platforms was influenced by the northeast direction of the trade winds), and most have 30 m eolianite ridges (direction of such ridges is impacted by seasonal wind patterns) (Carew and Mylorie, 1997). In the northern Bahamas, temperatures are subtropical temperate, but the climate becomes drier towards the south with declining tree size and a shift to the dominance of xeric plants (drought resistant) (Carew and Mylorie, 1997). Based on instrumental datasets, Jury et al. (2007) determined that islands northwest of Cat Island and Exuma receive >1400 mm yr^{-1} of rainfall, whereas those further to the southeast receive only 872 mm yr^{-1}. This precipitation change may in part explain why only the northern Bahamian islands are sufficiently mesic to support *Pinus* forests (Abaco, Andros, Grand Bahamas, New Providence) (van Hengstum et al., 2016).

Blackwood Sinkhole is located 220 m inland from the beach on the eastern shore of Great Abaco. Great Abaco is a low-lying carbonate island in the northern Bahamas, (26.79°N, 77.42°W) (van Hengstum et al., 2016) (Figure 1). Abaco displays high eolinatic ridges limited to the windward side of the island (Carew and Mylorie, 1997). Present-day vegetation in the Bahamas is described in two units (coppice and pineland/pineyard) (Steadman et al., 2007). The coppice (on nearby Andros island) is

broadly quantified as being dominated by an array of woody species (Steadman et al., 2007). Modern vegetation on Abaco island is supported by pine forest but includes a shrub layer including tropical hardwoods (poisonwood, *Metopium toxiferum*), cassada wood (*Bumelia salicifolia*), tetrazigia (*Tetrazigia bicolor*), five-finger (*Tabebuia bahamensis)* and quicksilver (*Thouinia discolor*) (Kjellmark, 1996).

A full suite of palynological data has been previously analyzed within Blackwood Sinkhole (van Hengstum et al., 2016), which indicates a shift in landscape vegetation dominance from tropical hardwoods (*Myrtaceae*) and palms (*Arecaceae*) to pines (*Pinus*) and mangroves (*Conocarpus*) at 1000 Cal yrs BP. These results are consistenet with Slayton (2010) who also documented a shift to the dominance of pines on the Abaco landscape at 1000 Cal yrs. BP.

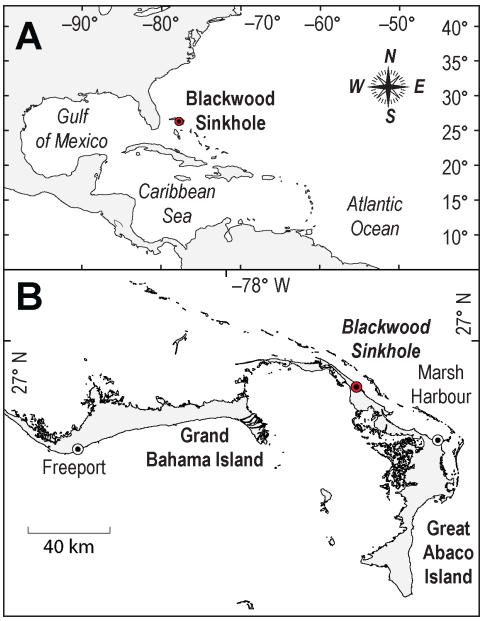

Figure 1: Map of BLWD-C2 and Bahamas Region. (A) Blackwood Sinkhole in the tropical North Atlantic Ocean and (B) the main islands on the Little Bahama Bank with Blackwood located on the eastern shore of Great Abaco island. Adapted after *van Hengstum et al.* (2016)

Blackwood Sinkhole is groundwater fed, and is stratified; anoxic saline groundwater is 15 to 40 m below sea level (van Hengstum et al., 2016). Towards the beach, the sinkhole is adjacent to a mangrove; on the other side, Blackwood is surrounded by pine forest (Figures 1, 2). Blackwood Sinkhole ranges from 33 to 38 m deep (110-126 feet) and approximately 32 m in diameter. The anoxic bottom water prevents bioturbation, which supports excellent sediment preservation potential within the basin (van Hengstum et al., 2016).

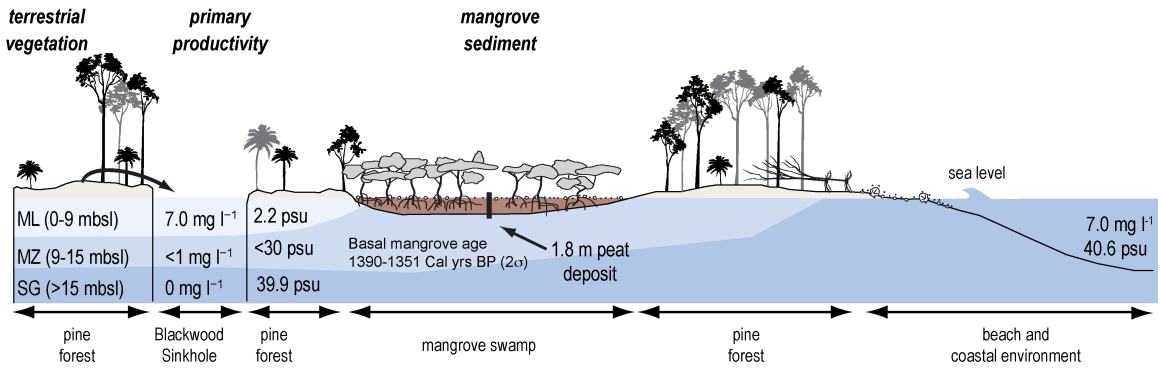

Figure 2: Conceptual Model of Sinkhole and Surrounding Vegetation. Adapted from (van Hengstum et al., 2016).

In 2011 and 2013, sediment push cores were taken from Blackwood Sinkhole using advanced technical scuba diving procedures. One core was taken from the center of the sinkhole basin (BLWD-C3, ~110 cm) and one was taken from the eastern margin (BLWD-C2, ~137 cm). Sinkhole cores terminate on carbonate gravel, but above the gravel (from the cores within the sinkholes), there is laminated gytija (1 mm to 1 cm laminae) interbedded with coarse-grained sedimentary layers (van Hengstum et al.,

2016). Sedimentation rate for BLWD-C2 was nearly constant through the late Holocene (van Hengstum et al., 2016). This allows for a high-resolution record of geochemical changes to be explored. An additional core was collected from the adjacent mangrove environment, terminating on eolianite bedrock (BLWD-C6, ~110 cm).

Coarse-grained sedimentary layers (indicative of hurricane overwash layers, from flooding caused by strong storms), interbedded with laminated gytija, correlates to an interval of elevated hurricane strikes on Abaco island during the last 3000 years, modulated by migrations of the ITCZ (van Hengstum et al*.,* 2016).

Within the sinkhole, the primary components of sediment include: OM from primary production, authigenic calcium carbonate production, erosional products from the surrounding landscape (karst fragments, terrestrial plant litter). Typical particles that would be characterized as a beach environment are currently lacking within the sedimentary record within the sinkhole (rounded marine mollusks, benthic foraminifera) (van Hengstum et al*.,* 2016). The lack of beach particulates, in combination with the rare occurance of marsh-based foraminifera (that would not be able to survive within the anoxic bottom of the sinkhole) and angular karst fragments suggests that the adjacent mangrove and surrounding terrestrial environment are the main sources of sedimentary supply (van Hengstum et al. 2016).

On Abaco Island, there is a history of colonization of Lucayan Indians, based on recovered remains and artifacts (Keegan, 1992; Kjellmark, 1995). There is additional data for charcoal counts (within the Blackwood cores), and mineral data (XRF) available, which will fully be explored in the future.

4. METHODS

4.1 Core Collection and Age Models

Sediment push cores were collected from Blackwood Sinkhole using technical scuba diving methods (BLWD-C2: 100 cm, BLWD-C3: 137 cm). A separate push core was located on the adjacent wetland between the beach and sinkhole site (BLWD-C6: 110 cm).

To generate age models for the cores, terrestrial plant macrofossils (twigs, leaves) were radiocarbon dated at the NOSAMS (National Ocean Sciences Accelerator Mass Spectrometry) facility at Woods Hole Oceanographic Institution. An age model was then computed using Bacon v 2.2 (Bayesian age-depth modeling software). The age-model of BLWD-C2 was generated previously (van Hengstum et al., 2016), as was the basal date of BLWD-C6. However, within this project, twigs and leaves were taken from 5 horizons within BLWD-C3.

4.2 Organic Geochemistry

All processing of samples was done with preparative cleaning of vials using 450°C (for four hours) combustion, and methanol (MeOH)/dichloromethane (DCM) rinsing to remove any excess organics, or contamination between samples. Sediment sub-samples were contiguously obtained downcore to characterize the geochemical variability with BLWD-C2 sub-sampled at 5 mm increments, BLWD-C3 sub-sampled at 1 cm increments, and BLWD-C6 sub-sampled at 2 cm increments. Sediment sub-samples were placed in combusted 20 mL scintillation vials and freeze-dried until all moisture

was removed. Freeze dried sediment was then homogenized using a mortar and pestle, and stored until further analysis.

4.2.1 Carbon, Nitrogen, $\delta^{13}C_{org}$ and $\delta^{15}N_{org}$ Analysis

First, Total Carbon (TC) and Total Nitrogen (TN), as weight percents, were determined on freeze-dried 5 mg bulk sediment samples introduced into a Costech 200 Elemental Analyzer (not acidified). Data calibration was determined relative to internal and international reference standards (e.g., acetanilide and standard reference material for marine sediments, NIST).

The determined TC of the bulk sediment was used to determine target weights (1-2% TC) for subsequent measurement of $\delta^{13}C_{org}$ and $\delta^{15}N_{org}$ values. Next, a 100 mg portion of sediment was directly acidified with 8 mL of 1M Hydrochloric Acid (HCl) for 24 hours, or until effervescence between carbonates and HCl ceased. Samples were then dessciated at 50°C, and re-homogenized using a mortar and pestle. Samples were acidified every-other 5 mm interval for BLWD-C2, every 1 cm for For BLWD-C3, and every 2 cm downcore for BLWD-C6. The $\delta^{13}C_{org}$ and $\delta^{15}N_{org}$ ratios of bulk organic matter, in addition to TC and TN of the acidified sediment sub-samples, were then measured at the Baylor University stable isotope laboratory on a Thermo-Electron Delta V Advantage Isotope Ratio Mass Spectrometer. Standards and calibrations were also simultaneously run on the GC-IRMS during $\delta^{13}C_{org}$ and $\delta^{15}N_{org}$ analysis. Final isotopic ratios are reported relative to the standard Vienna Pee Dee Belemnite (VPDB) in per mil (‰). The potential loss of carbon from the direct acidification process was corrected by multiplying the percent of sample remaining (post-acidification weight subtracted from

pre-acidification weight/pre-acidification weight) and the TC value measured after direct acidification (taken with isotopic measurements).

4.2.2 Multivariate Analysis and Mixing Model

A Principal Component Analysis (PCA) between cores and organic geochemical proxies measured was determined using *PAST* (PAleontological STastics)(Hammer et al., 2001). Various iterations of these groupings were explored. Because the proxies had different scientific units ($\delta^{13}C_{org}$, $\delta^{15}N_{org}$, C:N, OC), a correlating function was used in *PAST* to normalize the data (dividing by the standard deviation) to better represent relationships within the dataset. The plots that displayed the most-defined relationships were reported and used for further analysis. Blank data spaces (due to instrument, or analysis error) were infilled using a mean value generated by *PAST*.

A preliminary stable isotopic mixing model was created using three endmembers (selected from $\delta^{13}C_{org}$, C:N, and varying concentrations of both TN and OC) following methods by Phillips and Koch (2002) and Gonneea et al. (2004). $\delta^{13}C_{org}$, and C:N ratio endmembers were selected using a cross plot of C:N and $\delta^{13}C_{org}$ to find relationships between the datasets (Figure 8). Endmembers were selected relative to three source groupings within the cores (as both a function of time and variation of geochemical signals). The endmembers selected attempt to represent allochthonous (terrestrially-derived vegetation fluxed in, within group 3), autochthonous freshwater (produced within group 2), and a mixed interval of potential marine and terrestrial (or mangrove origin) (group 1) OM contributing to the system (Table 1) coherent to literature values (Lamb et al., 2006, and references therein).

Table 1: Mixing Model Endmembers. Endmembers selected for source contributions throughout the core, determined by the C:N versus $\delta^{13}C_{org}$ crossplot for the entire core.

Core	Interval	Group	$\delta^{13}C_{org(‰)}$	C:N	OC%	TN%
BLWD-C3	27-28cm	1	−25.4	15.7	12.0	0.9
BLWD-C2	34.5-35cm	2	−33.9	15.1	10.6	0.8
BLWD-C3	130-131cm	3	−26.1	48.9	20.1	0.5

Mass balance equations (Equation 1) of contributions for all three endmembers, according to stable isotopic parameters and subsequent concentrations of carbon and nitrogen can be written to understand source contributions to a mixture (Equations 1-5) (Phillips and Koch, 2002). Within this work, fractions and contributions were calculated relative to the fraction of carbon and $\delta^{13}C_{org}$. Phillips and Koch (2002) developed the following set of equations using matrix algebra to solve for $f_{X,B}$, $f_{Y,B}$, and $f_{Z,B.}$, where each parameter represents, respectively, the fraction of a particular source of biomass in the stable isotopic signal (Equation 3).

Equation 1: $\delta^{13}C_m$ of the mixture are defined by the sum of the fraction of the carbon multiplied by the selected end-member of the respective parameter ($^{13}C_{org}$), adapted from Phillips and Koch (2002).

$$\delta^{13}C_m = f_{X,C}\delta^{13}C_{X'} + f_{Y,C}\delta^{13}C_{Y'} + f_{Z,C}\delta^{13}C_{Z'}$$

Equation 2: Fractional contributions of the sources (in terms of carbon and assimilated biomass) are constrained to equal 1 (Phillips and Koch, 2002). Only the fraction of assimilated biomass and the fractional concentrations in terms of carbon were utilized in this project.

$$1 = f_X C + f_Y C + f_Z C$$

$$1 = f_X B + f_Y B + f_Z B$$

Equation 3: Fractional contributions of the assimilated biomass ($F=A^{-1}B$) are solved through the following matricies (taken directed from the equations displayed in Phillips and Koch, 2002). $\delta^{13}C_{orgX',Y'Z''}$, $C:N_{X',Y',Z'}$, and elemental concentrations of C and N are based on the endmembers selected. $\delta^{13}C_M$ and $C:M_m$ represent the mixture.

$$A = \begin{bmatrix} (\delta^{13}C'_X - \delta^{13}C_M) & \delta^{13}C'_Y - \delta^{13}C_M & \delta^{13}C'_Z - \delta^{13}C_M \\ (CN'_X - CN_M)N_X & (CN'_Y - CN_M)N_Y & (CN'_Z - CN_M)N_Z \\ 1 & 1 & 1 \end{bmatrix}$$

$$F = \begin{bmatrix} f_X B \\ f_Y B \\ f_Z B \end{bmatrix}$$

$$B = \begin{bmatrix} 0 \\ 0 \\ 1 \end{bmatrix}$$

$$F = A^{-1}B$$

Equation 4: Fractional contributions of each parameter ($f_{X,C}$, $f_{X,Y}$, $f_{X,B}$, and additionally for the y and z components) are solved from calculating the amount of assimilated

biomass in the mixture, relative to the elemental concentrations of the endmembers selected (Equation 3).

$$f_{X\,C} = \frac{f_{X\,B}[C]_X}{f_{X\,B}[C]_X + f_{YB}[C]_Y + f_{Z\,B}[C]_Z}$$

$$f_{Y\,C} = \frac{f_{Y\,B}[C]_Y}{f_{X\,B}[C]_X + f_{YB}[C]_Y + f_{Z\,B}[C]_Z}$$

$$f_{Z\,C} = \frac{f_{Z\,B}[C]_Z}{f_{X\,B}[C]_X + f_{YB}[C]_Y + f_{Z\,B}[C]_Z}$$

Equation 5: A tolerance interval of the model can expand the validity and variation in the dataset, defined in Dittmar et al. (2001) as the following. τ is the tolerance, a^1, b^1, c^1 represents the expanded validity of the end-member (by 15%), and a, b, c is the strict validity of the model (endmembers) (Table 1)

$$\tau = \frac{a^1}{a}100\% = \frac{b^1}{b}100\% = \frac{c^1}{c}100\%$$

After ensuring that Equations 1-5 fit the endmembers selected (Table 1), a Python script was developed to apply the above equation for all of the data in BLWD-C2 and BLWD-C3, (*n*=237). Negative output values from the model can represent diagenetic alteration of the samples, or a contribution from a source not defined by the three endmembers (Dittmar et al., 2001; Gonneea et al., 2004). To expand the validity of the model, a tolerance interval was applied (Equation 5) and added or subtracted to endmembers to expand a triangular plot that was created using the named endmembers (Table 1). To test validity of the model and the applied tolerance interval, measured $\delta^{13}C_{org}$ signatures were plotted against the predicted $\delta^{13}C_{org}$ (calculated using Equation 1) and displayed an r^2 value of .78.

4.3 Oxidation, Extraction and Quantification of Lignin-Derived CuO Oxidation Products

The method to extract and quantify free lignin phenols from the bulk organic sedimentary matter within Blackwood Sinkhole was adapted from Hedges and Ertel (1982) and Louchouarn et al. (2010). Sediment samples (n=34, at about a 3 cm resolution throughout the core) were run concurrently through oxidation, extraction and quantification with a marine sediment standard reference material (Louchouarn et al., 2010). Additionally, a surrogate standard was used relative to quantification on the GC-MS at TAMUG.

Lignin reaction vessels were filled with a metal ball, 150 ± 4 mg ferrous ammonium sulfate, 330 ± 4 mg of cupric oxide, and enough sediment to match 1−3 mg of OC into each bomb. Vessels were placed in a carousel, filled to brim (1-2.5 mL) with 2N Sodium Hydroxide (NaOH) and sparged with Argon gas for 45 minutes (at 5 mL/min) (to ensure that no oxygen was contained within the vessels).

Samples were placed into a GC oven fitted with an internal rotating rack, and rotated for 150 minutes reaching an oven temperature of 154°C (ramping at 4.2°C/min for 30 minutes). After samples were completely cooled, each sample was spiked with 50 μL of external standard, d-7 Cinnamic Acid (250 ng/μL concentration), and centrifuged for 5 minutes. Vessel contents were decanted (using combusted Pasteur pipettes) into 40 mL centrifuge tubes. Vessels were then re-filled with 1N NaOH, centrifuged and decanted. This was repeated for a total of 3 extractions of NaOH.

After a final rinse of NaOH, 2.5 mL of 6N HCl was added to the centrifuge tubes, until samples were a pH of 1 or less (this was tested with pH paper after vortexing tube for 30 seconds). 3 mL of ethyl acetate was added to each sample and was vortexed for 1 minute. Samples were then centrifuged (6 samples at a time) for 5 mins, for a total of 3 extractions. The ethyl acetate aliquot layer was pipetted and expelled in a 20 mL combusted vial after each centrifugation for a total of 9 mL ethyl acetate.

Samples were then chemically dried (to remove any water that could have remained in the samples) using combusted sodium sulfate until saturation was reached (crystals were free moving, not lumpy). The remaining ethyl acetate was pipetted into 15 mL conical vials.

Conical vials were placed into a Centrivap and dried at 45°C (taking care to not allow samples to remain in the centrivap for a long time because of volatilization). Dried samples were re-suspended in two turns with 400 μL of pyridine. Samples were then diluted in a 50:500 μL ratio of sample:pyridine.

Samples were prepared for preparation on the Varian triple quadrupole 480-300 gas chromatography-mass spectrometry (GC-MS) system. 50 μL of the diluted sample was added with 50 μL of derivatizing agent, 99:1 BFSTA:TMCS (N_3O-bis(trimthylzilyl)trifluoroacetamide, containing 1% trimethylchlorosilane), and 50 μL d7 CiAd internal standard. Standards were prepared through using 50 μL of BFSTA, 50 μL of d7 CiAd (surrogate standard), and 50 μL of diluted sample. Standards were prepared with 50 μL of BFSTA, 50 μL of d7 CiAd (internal standard), and 50 μL of a internally prepared LOP calibration solution (1.0 ng/μL). Samples and standards were heated in a

20-wells block heater at 75°C for 30 mins for full derivatiziation before they were injected. The GC-MS was equipped with a fused silica column (J&W DB-5MS, 30 m x 0.25 mm i.d., 0.25 um film thickness (Agilent Technologies, Santa Clara, CA, USA)). The following products were analyzed and reported: p-OH Benzaldehyde, p-OH Acetophenone, d7-Anisic Acid, Vanillin, d7-Trans-Cinnamic Acid, Acetovanillone, p-OH Benzoic Acid, Syringaldehyde, Vanillic Acid, Acetosyringone, 3,5 diOH Benzoic Acid, Syringic Acid, p-Coumaric Acid, Ferulic Acid.

5. RESULTS

5.1 Age Model Results

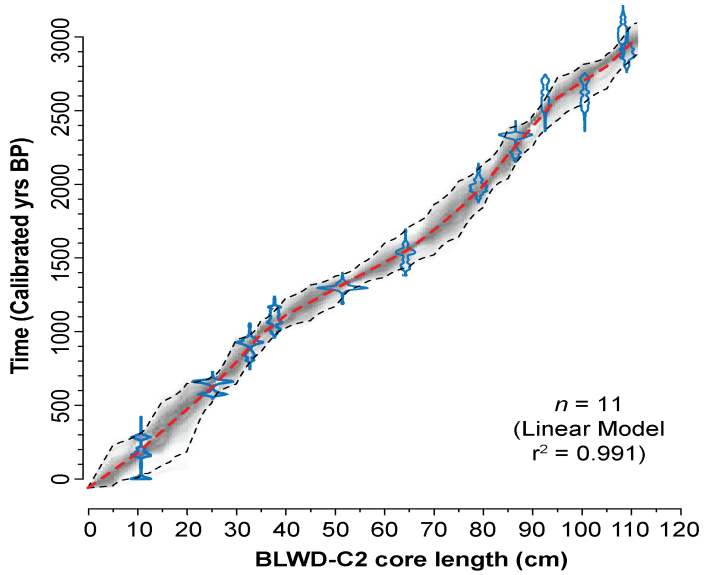

Figure 3: Age Model of BLWD-C2. This was created using Bacon v2.2 adapted from work contributing to van Hengstum et al., 2006.

BLWD-C6 records approximately 1400 years of sedimentation within the mangrove, according to one basal radiocarbon date. BLWD-C2 records a near-linear accumulation of sediment, for approximately 3000 years (Figure 3) (van Hengstum et al, 2016). BLWD-C3 records approximately 1700 years of sedimentation.

5.2 $\delta^{13}C_{org}$ and $\delta^{15}N_{org}$ Signatures, C:N Ratio, OC

For measurements of TC and TN (performed at TAMUG), replicates yield a mean precision of 1.9%. For $\delta^{13}C_{org}$ and $\delta^{15}N_{org}$ signatures (and additional measurement of TC and TN of the acidified fraction) measured at Baylor, replicates are within a yielded a mean precision of 5.0%.

Table 2: Mean Geochemical Proxies for BLWD-C2,BLWD-C3**.** Mean values of $\delta^{15}N_{org,}$ $\delta^{13}C_{org}$, C:N ratio and OC for BLWD-C2 and BLWD-C3. Standard deviations were calculated relative to the individuals displayed as *n*.

Core	Group	Interval (YBP)	*n*	$\delta^{13}C_{org(‰)}$	$\delta^{15}N_{org(‰)}$	C:N	OC(%)
BLWD-C2	1	0-1008	35	−28.0 ± −1.8	2.2 ± 1.0	19.3 ± 3.9	10.9 ±3.5
BLWD-C2	2	1039-1503	25	−30.9 ± −1.6	4.7 ± .6	23 ± 10.8	10.3 ± 5.8
BLWD-C2	3	1520-2990	50	−30.3 ± −1.6	3.2 ± .9	29.4 ± 17.3	11.3 ± 4.0
BLWD-C3	1	0-973	73	−27.3 ± −0.8	1.2 ± .8	19.8 ± 3.1	10.9 ± 2.3
BLWD-C3	2	1077-1497	36	−29.5 ± −2.8	3.4 ± .8	28.3 ± 8.4	16.3 ± 5.6
BLWD-C3	3	1508-1738	18	−27.6 ± −1.4	2.3 ± 1.2	43 ± 14.2	20.3 ± 7.1

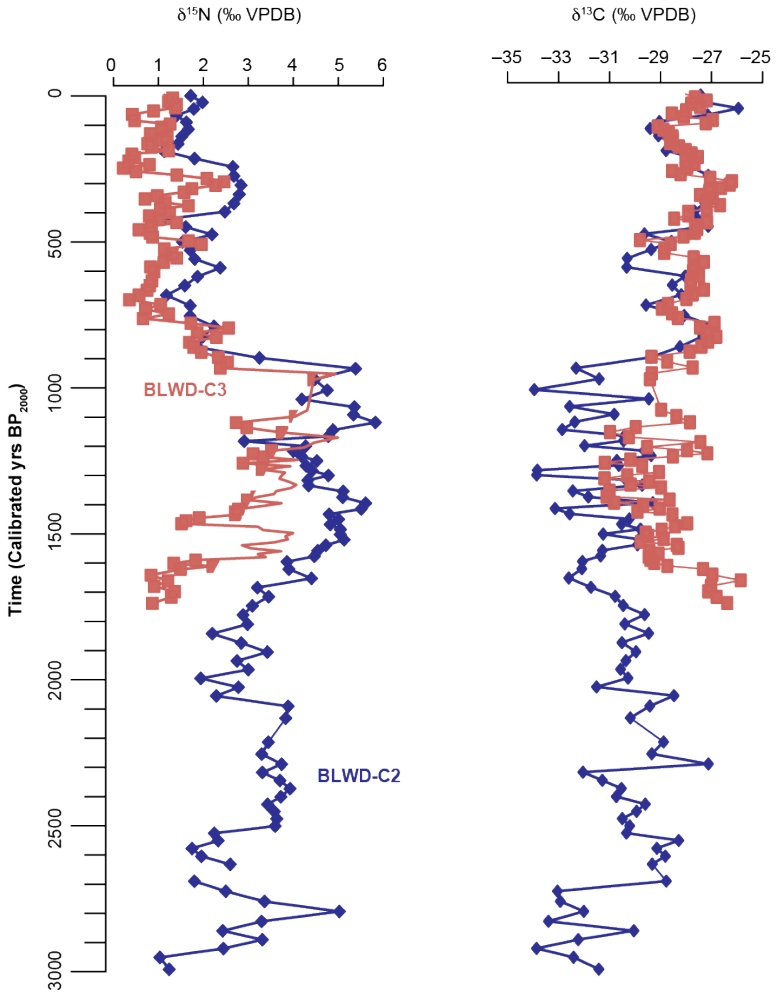

Figure 4: Isotopic Consistency within Blackwood Sinkhole. Downcore representation of $\delta^{15}N_{org}$ and $\delta^{13}C_{org}$ values in BLWD-C2 and BLWD-C3.

At approximately 826 Cal yrs BP within BLWD-C2, and 828 Cal yrs BP within BLWD-C3 (when *Pinus* starts to dominate), $\delta^{13}C_{org}$ values are within 2.16% between cores, while $\delta^{15}N_{org}$ values are within 14.15% (Figure 4)

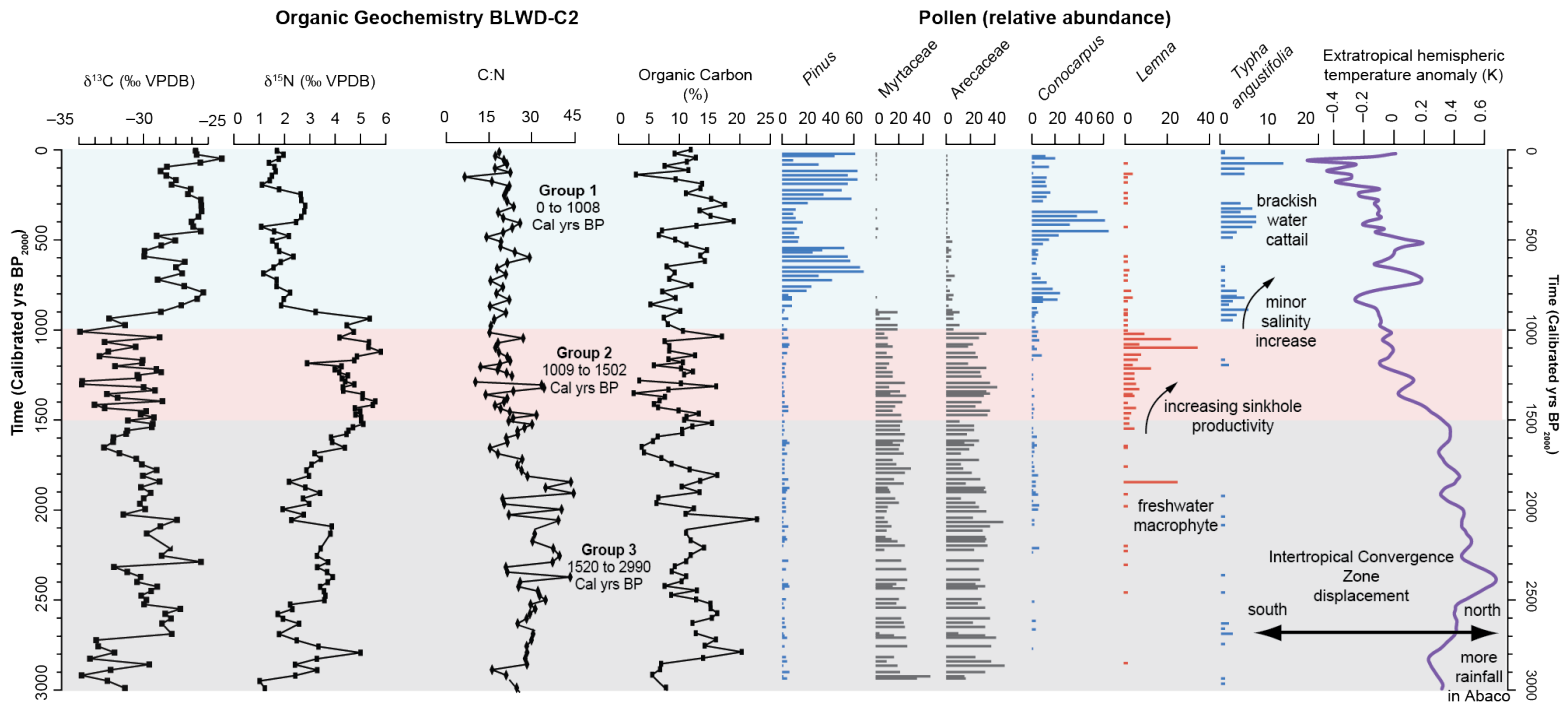

Figure 5: Organic Geochemical Proxies (Pollen and Climate Added), BLWD-C2. Palynological data was adapted from (van Hengstum et al., 2016), and the extratropical interhemispheric temperature anomaly from (Schneider et al., 2014). Both are included to infer possible trends between meridional ITCZ shifts and geochemical and palynological trends.

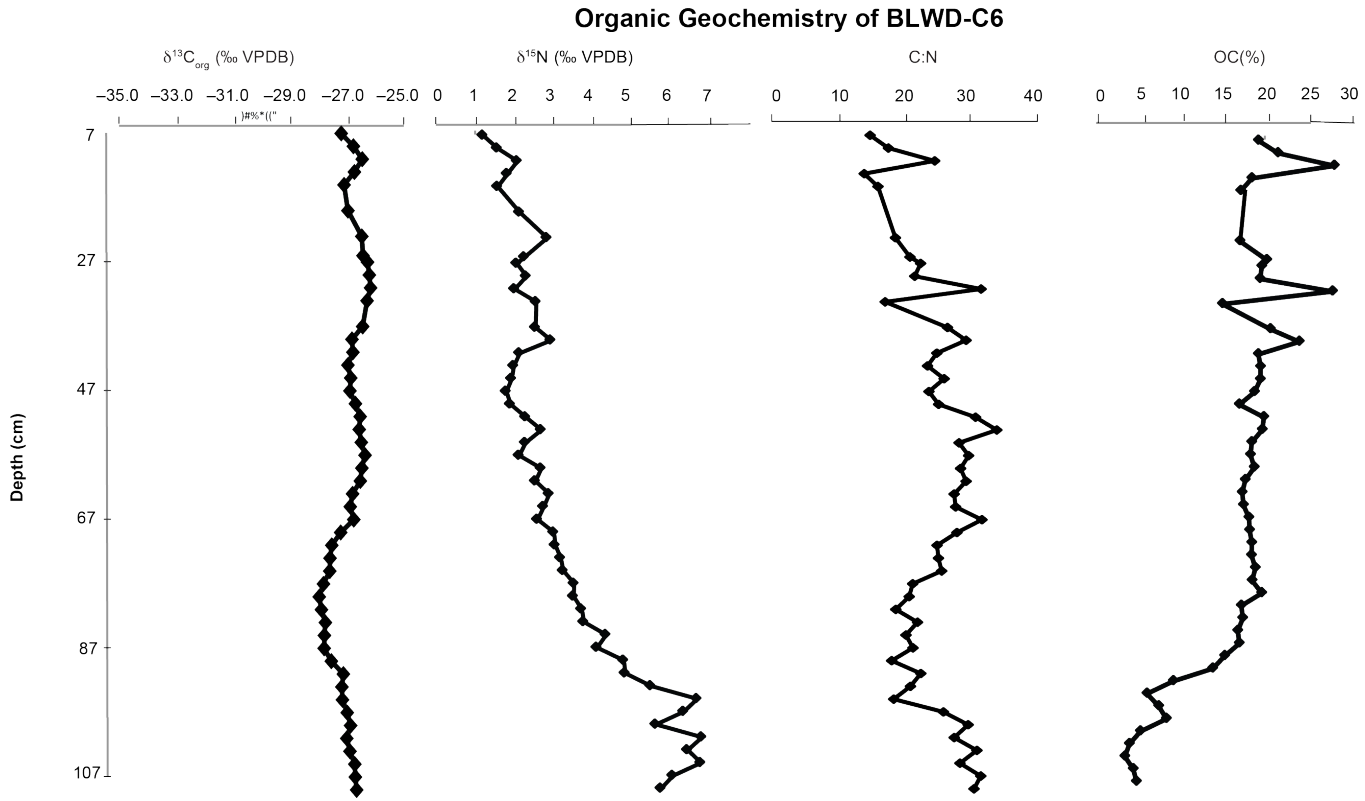

Figure 6: Organic Geochemical Proxies for BLWD-C6. Organic geochemical proxies ($\delta^{13}C_{org}$, $\delta^{15}N_{org,}$ TN(%), C:N, OC (%) measured for BLWD-C6 (n = 49). This data is plotted with respect to depth because only one radiocarbon date was obtained for BLWD-C6 (a basal date of ~1350 Cal yrs BP).

5.2.1 Multivariate Analysis and Three Endmember Mixing Model

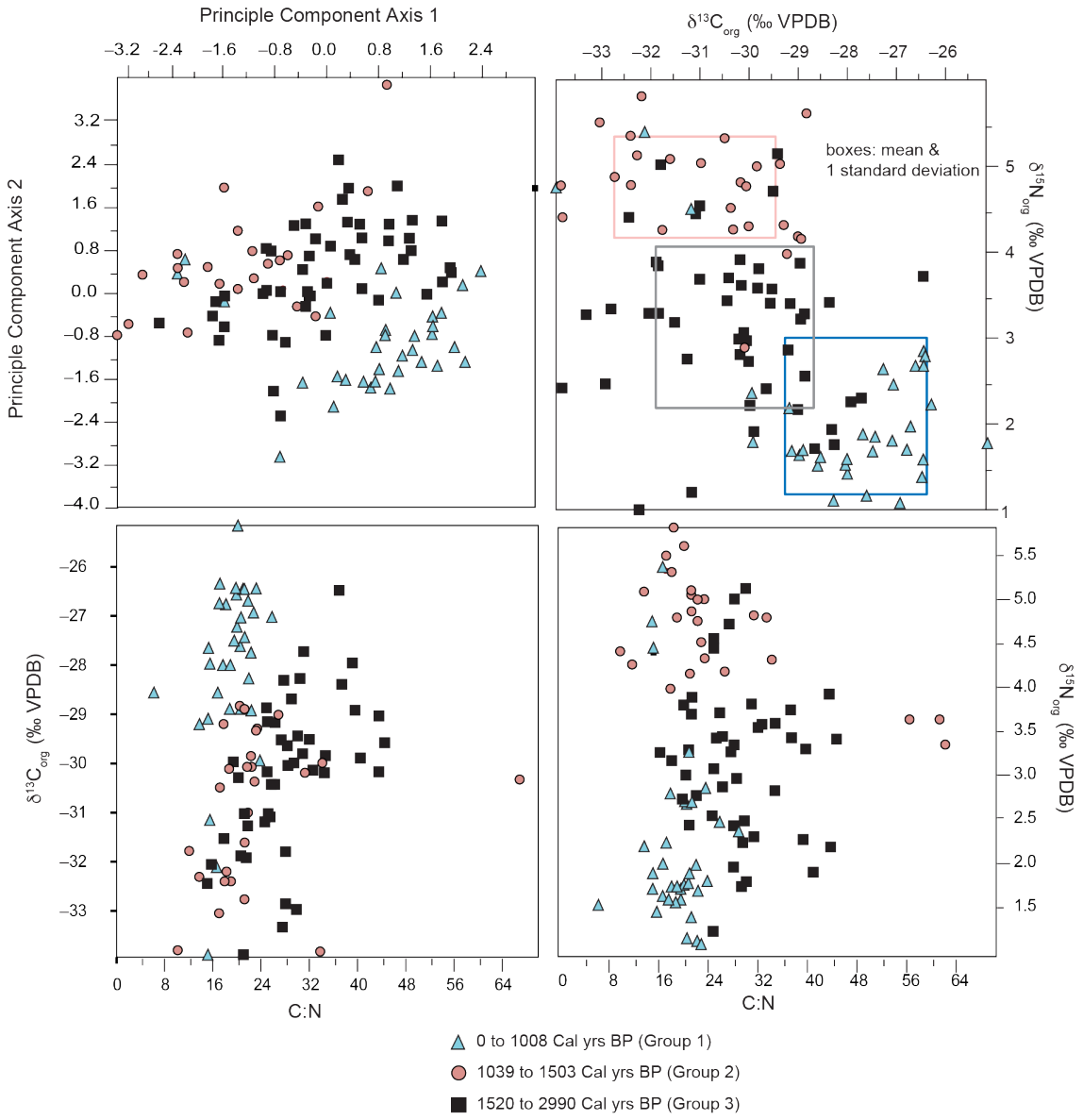

Figure 7: Source Correlation for BLWD-C2. For Group 1, *n*=35, Group 2, *n*=25 and Group 3, *n*=50. (Upper Left) Results of Principle Component Analysis (PCA) on $\delta^{15}N_{org,}$ $\delta^{13}C_{org}$, C:N ratio and OC. PC1 accounts for 46.9% of variance, while PC2 accounts for 33.1% of variance within analysis. (Upper Right) Cross plot between $\delta^{15}N_{org}$ and $\delta^{13}C_{org}$, plotted with 1 standard deviation. (Lower Left) Cross plot between $\delta^{13}C_{org}$ and C:N ratio. (Lower Right) Cross plot between $\delta^{15}N_{org}$ and C:N ratio primary geochemical proxies.

Average $\delta^{13}C_{org}$ within the mangrove core is −26.9‰ ± −.5 and average $\delta^{15}N_{org}$ is 3.3‰ ± 1.6 (Figure 6). Isotopic evidence, C:N and OC was plotted with pollen and climate data (van Hengstum et al. 2016; Schneider et al. 2014) Figure 5). An anomalous data point within the C:N (a value of approximately 66) ratio at ~1400 Cal yrs BP was removed for scale of the C:N plot with time.

PCA and subsequent cross plots revealed three groupings of OM within Blackwood-C2 (Fig. 6). Group 1, *n*=35, Group 2, *n*=25 and Group 3, *n*=50. PCA of BLWD C2 was created using $\delta^{13}C_{org}$, $\delta^{15}N_{org,}$ OC(%) and C:N signatures. Variance of Principal Component 1 (PC1) was 45.1%, while variance of Principal Component 2 (PC2) was 32.8%. PCA of the entire set of data (BLWD-C2, C3, C6) (*n*=286) was created using $\delta^{13}C_{org}$, $\delta^{15}N_{org}$, OC and C:N signatures. Variance of PC1 was 39.8%, while variance of PC2 was 30.5% (Fig. 7). Distinct groupings (Groups 1, 2, and 3) were colored for the entire data set, based on the patterns (and corresponding time intervals) found within BLWD-C2 (Figure 6), but were subdivided (with additional changes in color) between cores. Within BLWD-C3, Group 1, *n*=73, Group 2, *n*=36 and Group 3, *n*=18. The entirety of BLWD-C6 was treated as a group, *n*=49. The groupings that were developed through the exploratory PCA and cross plots are further used to describe intervals of data changes throughout this thesis.

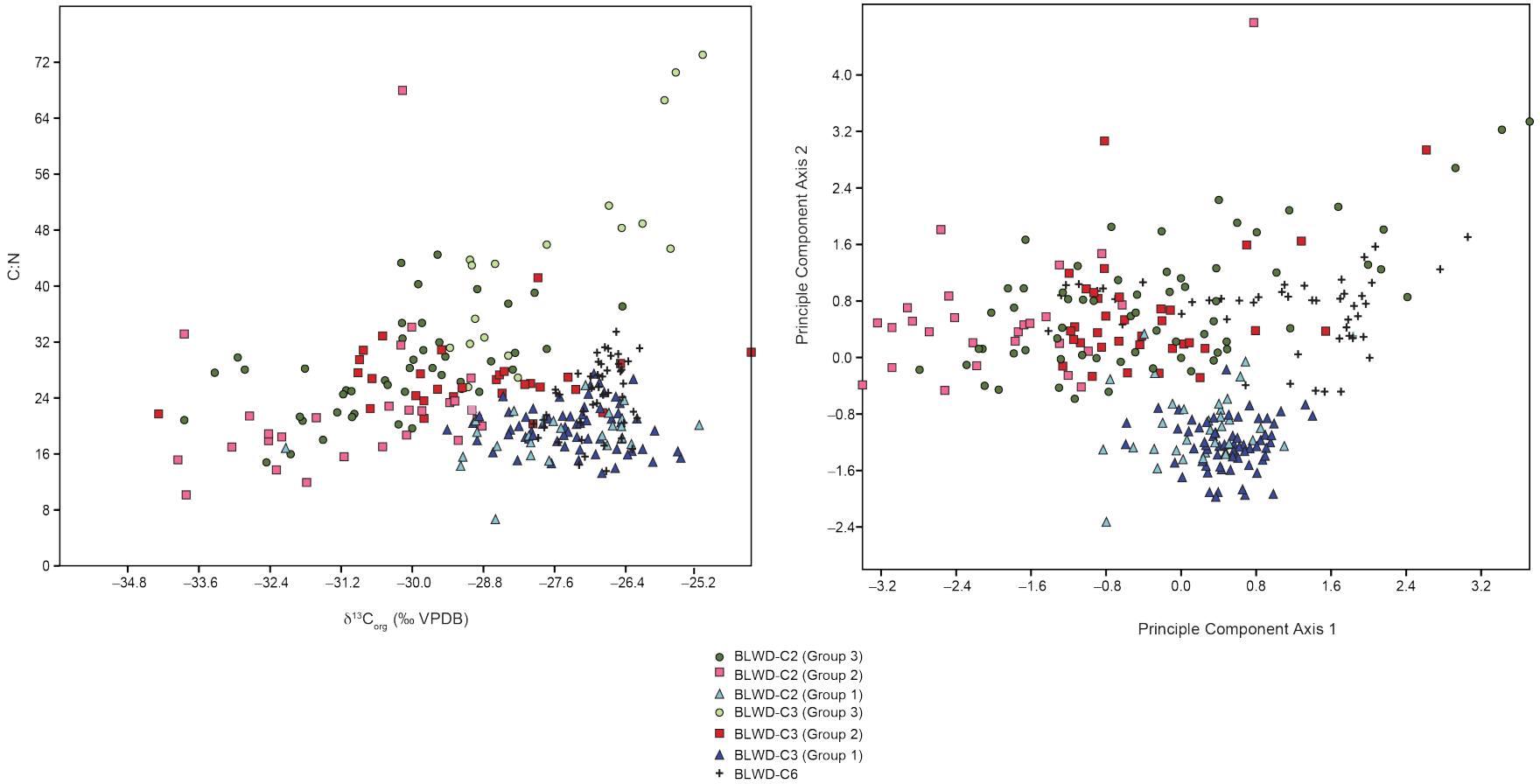

Figure 8: Source Correlation for BLWD-C2,C3,C6**.** $\delta^{15}N_{org,}$ $\delta^{13}C_{org}$, C:N ratio and OC data from BLWD-C2,C3,C6. *n*=286 (BLWD-C6, *n*=49; BLWD-C3, *n*=127, BLWD-C2, *n*=110). The color key on the bottom of the figure represents the color codes for all of the groupings within the subsequent cores. Number of individuals and average values of geochemical proxies within each group can be found in Table 2. Left XY plot is a cross plot of C:N ratio versus $\delta^{13}C_{org.}$ Right XY plot is PCA results of the entire data set (PC2 versus PC1). Variance of PC1 is 39.8%, and 30.5% for PC2.

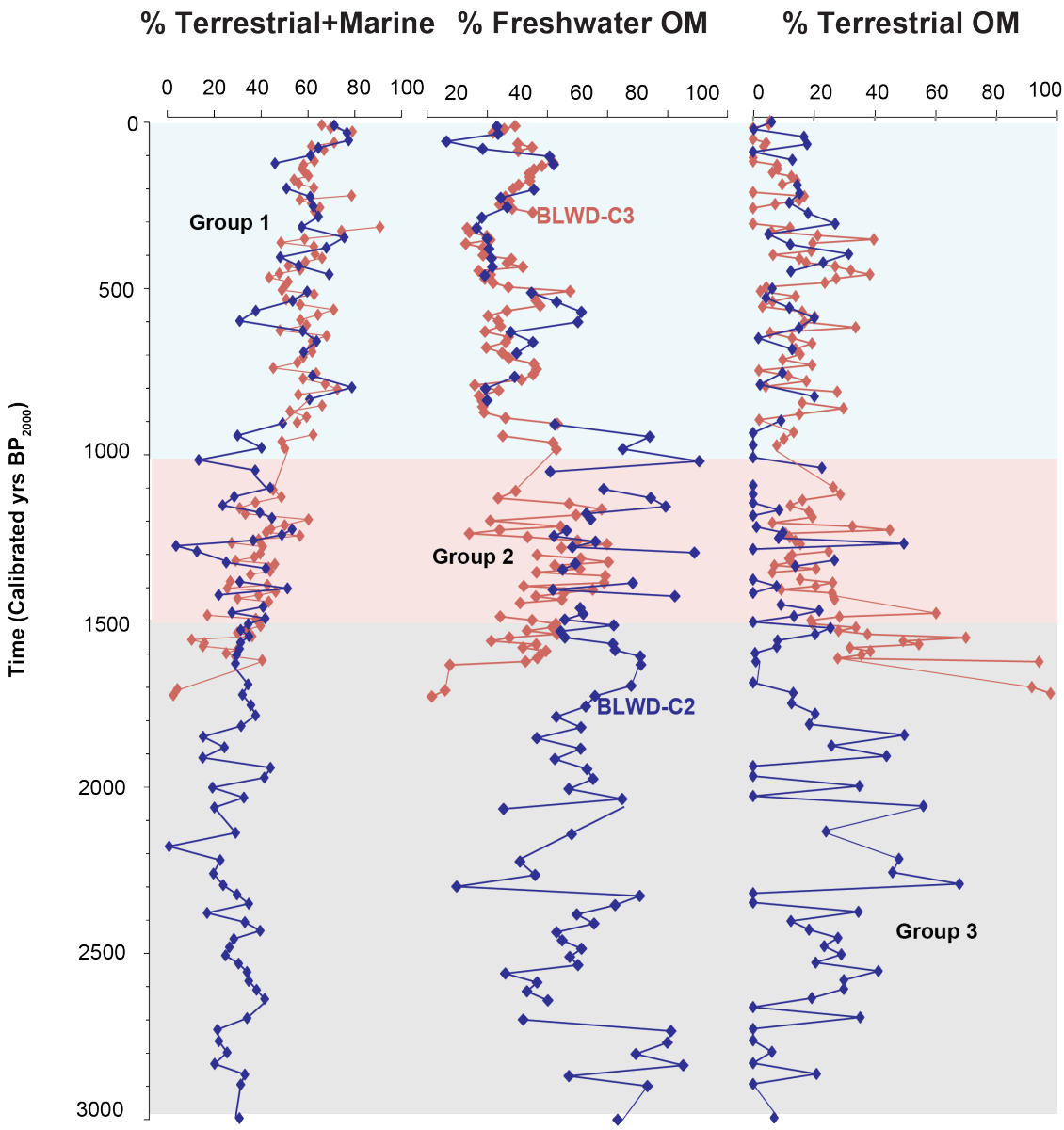

Figure 9: Mixing Model Results Fractions (%). Fractions as percentages, relative to carbon, calculated from the biomass fraction, according to the mixing model (Equations 1-5). % Terrestrial+Marine is indicative of the fraction of OM correlating to the Terrestrial+ Marine end-member (Group 1). % Freshwater OM is indicative of the fraction of OM correlating to the Freshwater OM end-member (Group 2). % Terrestrial OM is indicative of the fraction of OM correlating to the Terrestrial (Group 3). Endmembers are defined in Table 1.

The fractions of mixtures calculated (relative to the carbon in the samples) arerecorded as fractions of the mixtures based on the endmembers 1,2,3 (mixed terrestrial and marine, freshwater productivity, and terrestrial input, respectively) (Table 3; Figure 9). Group 1 is also named as Fc(marine + terrestrial), Group 2 as Fc(freshwater productivity) and Fc(terrestrial). These namings are consistent with literature values (Lamb et al., 2006). Group 1 shows the highest mean Fc(marine + terrestrial) percentages within the group 1 interval of both BLWD-C2 and BLWD-C3. Group 2 shows the highest mean Fc(freshwater OM) within the group 2 interval of both BLWD-C2 and BLWD-C3, except Group 2 of BLWD-C2 shows an equal percentage contributing form the marine+terrestrial end-member. Group 3 shows the highest mean Fc(terrestrial) within the group 3 interval of BLWD-C2. (Table 3, Figure 9).

Table 3: Fractions of Isotopic Mixing for BLWD-C2, BLWD-C3. Standard deviations were calculated relative to the number of horizons that fit the tolerance interval. Approximately 85% of the data fit the model with the 15% tolerance interval applied. Fraction/Percentages were calculated using Equations 1-5.

Core	Group	Interval (YBP)	$F_{C(marine+terr.)}$	$F_{C(fresh.\ prod)}$	$F_{C(terrestrial)}$
BLWD-C2	1	0-1008	61 ± 9	26 ± 8	13 ± 10
BLWD-C2	2	1039-1503	39 ± 9	40 ± 13	20 ± 12
BLWD-C2	3	1520-2990	22 ± 14	27 ±14	51 ± 27
BLWD-C3	1	0-973	57 ± 15	32 ± 19	11 ± 8
BLWD-C3	2	1077-1497	34 ± 13	56 ± 15	10 ± 13
BLWD-C3	3	1508-1738	29 ± 7	51 ± 16	20 ± 18

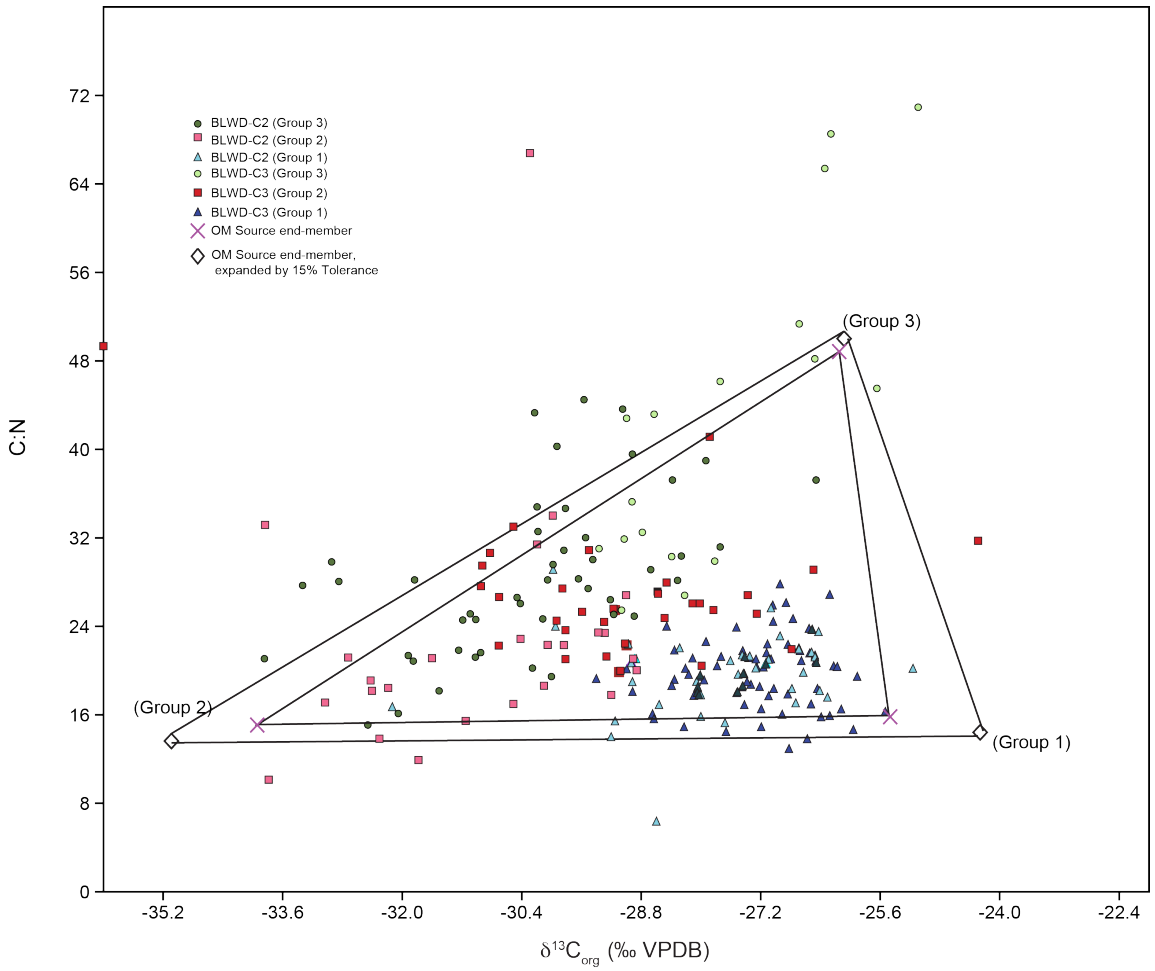

Figure 10: Triangle Plot with Endmembers, BLWD-C2, BLWD-C3. Cross plot of C:N and $\delta^{13}C_{org}$ values for BLWD-C2 and BLWD-C3. Endmembers are described in Table 1, expanded endmembers with a 15% tolerance is included in this diagram. The expanded endmembers for this figure were taken as a measure of 15% of both parameters (C:N and $\delta^{13}C_{org}$) , divided by the accepted endmembers (Table 1) and subsequent values were then added or subtracted to endmembers to expand the triangular space. The expanded group 1 end-member was 14.84, -24.59. The expanded group 2 end-member was 12.83, -34.79. The expanded group 3 end-member was 50.0, -26.1.

Approximately 70% of the data fits within the endmembers selected (Table 1), with a 15% tolerance interval added (Equation 5), approximately 85% of the data is

included in the expanded triangle (Figure 10). Most of the variation is based on horizons in groups 2 and 3 not fitting the model.

5.3 Lignin-derived CuO Products

Yielded replicates display a mean precision of 7.2% through oxidation, extraction and quantification of lignin phenols. Mean S/V values are lowest 0-1000 Cal yrs BP. There is consistent representation of Λ8 throughout the entire core. Intervals of increased Λ8, S/V, C/V, and Ad/Al(v) are consistent within the 1500-1000 Cal yr BP interval (Table 4, Figure 11).

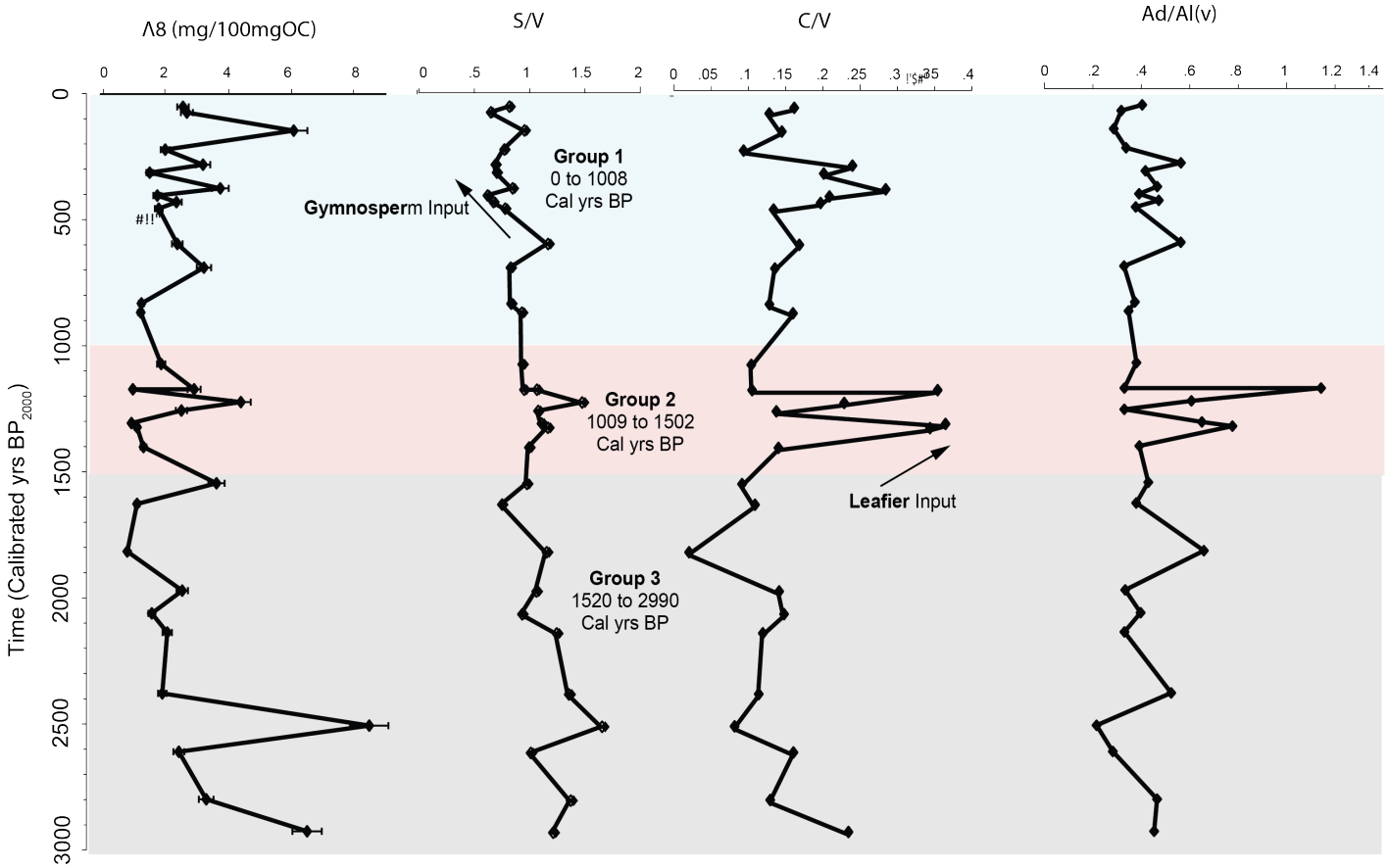

Figure 11: LOP of BLWD-C2. Lamda8 (mg/100mgOC), S/V (ratio of syringyl to vanillyl phenols), C/V (ratio of cinnamyl/vannilyl phenols), and the Ad/Al (v) (ratio of the Acid to Aldehyde products, relative to the vanillyl phenols). Groupings are further described in Table 3.

Table 4: Ligin Phenol Yields for BLWD-C2. Lignin Phenol yields for sedimentary horizons taken from BLWD-C2. This is the data that represents the most trustable yields, through using 1mg-3mg OC at the beginning of the oxidation process.

Core	Group	Interval (YBP)	*n*	Λ8	S/V	C/V	$Ad/Al_{(v)}$
BLWD-C2	1	0-1066	16	2.5 ± 1.3	0.8 ± .2	.2 ± .1	.3 ± .1
BLWD-C2	2	1166-1395	8	2.0 ± 1.2	1.1 ± .2	.2 ± .1	.3 ± .1
BLWD-C2	3	1539-2919	10	3.1 ± 2.4	1.2 ± .3	.1 ± .1	.3 ± .1

6. DISCUSSION

6.1 Temporal and Spatial Variability in Organic Matter Sedimentation

The provenance of organic matter deposited in the sinkhole is variable in time and space based on cross plots ($\delta^{13}C_{org}$ versus $\delta^{15}N_{org}$, $\delta^{13}C_{org}$ versus C:N), principal component analyses of the geochemical proxies ($\delta^{13}C_{org}$, $\delta^{15}N_{org}$, C:N, OC), and the 3-endmember mixing model. In general, three distinct intervals of time during the late Holocene were characterized by the dominance of different organic matter sources. From 1500 to 3000 Cal yrs BP, organic matter sedimentation was dominated by ~60% terrestrial organic matter in both cores. Organic matter sedimentation from 1000 to 1500 Cal yrs BP was likely dominated by inputs from high primary productivity in a freshwater environment, for example, ~56% of OM was derived from freshwater sources within BLWD-C3. Lastly, both marine and terrestrial sources of organic matter accumulated from 0 to 1000 Cal yrs BP (~51% within BLWD-C2), but marine-derived inputs were likely dominant from the adjacent mangrove environment. Both of the sinkhole cores exhibited very similar overall downcore trends, but there are notable differences (Fig. 4). For example, there is an offset in the absolute value of the $\delta^{15}N_{org}$ data between BLWD-C2 and BLWD-C3 of ~3.0‰. This is perhaps related to proximal location of BLWD-C2 to the sinkhole periphery. When compared to the sinkhole center (BLWD-C3), the periphery is more likely to receive sediment from the adjacent soil surface, and degradation within soil organic matter leads to slightly more enriched $\delta^{15}N_{org}$ values than the terrestrial organic matter source from where it derived (Natelhoffer and Fry, 1988). The $\delta^{13}C_{org}$ values of BLWD-C2 are also slightly more

depleted than BLWD-C3, by ~3-5‰, especially during the period from 15000 to 1000 Cal yrs BP.

This interpretation of a changing OM through time requires a few assumptions: that the sinkhole geomorphology remains constant through time, the amount of primary productivity is large enough in the sinkhole to record a signature, and that terrestrial vegetation immediately surrounding the sinkhole is indeed being fluxed into the basin. Given the frequency of hurricane events in the tropical north Atlantic, this latter assumption is likely valid. Sedimentary evidence suggests that no major geomorphologic changes occurred within the sinkhole throughout the late Holocene. However, geomorphological variation of Blackwood Sinkhole can be explored through additional surveys completed on the bottom of the sinkhole and the surrounding area. Addition surface samples from the surrounding landscape could also be analyzed to better understand OM sources. Estimates of primary productivity could also be explored through modern measurements of the meteoric layer (although there are limitations to such measurements, primary productivity estimates have been made based on methods including a water sampler, irradiance, incubations, filtering, and eventual quantification of chlorophyll measurements (Gieskes et al., 1979)). Despite these assumptions and the minor site-specific sedimentation patterns impacting the OM deposited at the periphery vs. center of this this small karst basin, there is an overall consistency in the observed downcore geochemical trends. As such, these consistent geochemical trends are likely reflecting broader environmental change on the surrounding landscape and in the sinkhole.

6.2 Terrestrial Organic Matter Dominance From 1500 to 3000 Cal yrs BP (Group 3)

Within a local paleoenvironmental context, the provenance of organic matter during the earliest part of the record must also have been derived from either aquatic productivity in the sinkhole itself or the adjacent forest ecosystem. Indeed, there is currently a large wetland environment within the adjacent topographic depression on the antecedent Pleistocene carbonate (constructional basin of Park Boush et al., 2014), but the pollen evidence suggests that this wetland was not established until ~1000 Cal yrs BP based on the an increase in *Conocarpus* (Fig. 5, van Hengstum et al., 2016). This earliest period of the geochemical record is mainly based on BLWD-C2 because the BLWD-C3 record extends only until 1700 Cal yrs BP. It is possible that the sinkhole periphery (i.e., BLWD C2) was more sensitive to deposition of terrestrial organic matter particles from the adjacent landscape. Furthermore, terrestrial organic matter input would likely have been enhanced at this time by hurricane overwash events, since coarse-grained sedimentation into Blackwood Sinkhole indicates that Abaco Island experienced elevated intense hurricane activity from 2600 to 1000 Cal yrs BP (van Hengstum et al., 2016).

The detailed geochemical evidence also indicates that the organic matter accumulating in Blackwood Sinkhole from 1500 to 3000 Cal yrs BP was most likely dominated by terrestrial sources, not aquatic (either freshwater or marine). More specifically, the LOP analysis indicates that angiosperm-sourced organic matter dominated sedimentation from 3000 to 1000 Cal yrs BP based on a higher mean S/V

ratio (Hedges and Mann, 1979) (Table 4). Mean C:N values are highest within this interval, and by comparison with literature values of C:N, $\delta^{15}N_{org}$ and $\delta^{13}C_{org}$ values, high C:N values are consistent with organic matter derived from terrestrial plants (Thornton and McManus, 1994; Ogrinc et al., 2005; Lamb et al. 2006 and references therein). The C/V ratio, which is a marker of soft tissues like leafy inputs from angiosperms, is not high during this interval, and $\delta^{15}N_{org}$, $\delta^{13}C_{org,}$ C:N signatures are not reflective of primary productivity in the basin itself (see Group 2 below), indicating that the OM deposited during this interval was indeed from the surrounding forest. Independent evidence from the previously compiled palynological data from BLWD-C2 indicate that during this time interval the landscape adjacent to Blackwood Sinkhole was dominated by tropical hardwoods (e.g., *Myrtaceae*) and palms (*Arecaceae*) (Figure 5). Furthermore, pollen evidence from a bluehole elsewhere in Abaco (Emerald Pond: Slayton, 2010) also indicates that tropical hardwoods dominated the landscape at this time. Therefore, the geochemical evidence for the dominance of terrestrial organic matter deposition in Blackwood Sinkhole accords with the independent evidence for island forest ecology.

6.3 Elevated Aquatic Productivity from 1000 to 1500 Cal Yrs BP (Group 2)

From 1500 to 1000 Cal yrs BP, the organic geochemical data indicate that aquatic primary productivity increased to the point where freshwater phytoplankton debris was the dominant contributor to deposited organic matter (Fig. 8). This is evidenced by consistent geochemical signals in both the sinkhole periphery (BLWD-C2) and center (BLWD-C3). The depleted $\delta^{13}C_{org}$ values could be indicative of either

terrestrial or freshwater phytoplankton organic matter sources (Table 2). However, the upcore trend to more enriched $\delta^{15}N_{org}$ values, in both cores, is consistent with aquatic primary producers. An increase in primary productivity from more eutrophic conditions within the sinkhole could progressively fractionate the residual dissolved inorganic nitrogen (DIN) pool in the sinkhole (Talbot and Laerderal, 2000; Brandenberger et al., 2011). The Cinnamyl/Vanillyl (C/V ratio) also markedly increases during this time, which is indicative of increased soft plant tissue deposition (derived from leafy plant inputs) (Hedges and Mann, 1979; Louchouarn et al., 1991). Based on the pollen evidence, the freshwater macrophyte, *Lemna* (considered an angiosperm), dominates at this time, which also suggests abundant nutrient availability. Additional biomarker analysis may be able to document freshwater eutrophication, such as lipids that are authentic to specific algae or eutrophic indicators (e.g., cholesterol: Makou et al., 2010; Zimmerman and Canuel, 2002)).

These geochemical and pollen results suggest that hydrologic conditions or nutrient availability changed in the sinkhole. Considering that the pollen results indicate no significant contemporaneous change in forest ecology, hydrographic changes must have been occurring in the sinkhole to alter primary productivity. Currently, the upper meteoric lens in Blackwood Sinkhole, which has a salinity of 2.2 psu, is continually recharged by precipitation and is continually discharging into the coastal zone in response to gravitational and buoyant forcing. Assuming that similar hydrogeological forcing conditions also operated in the past, an increase in primary productivity suggests

an increase in nutrient residence time in the sinkhole basin, or an increase in nutrient delivery in the basin to support elevated primary productivity.

6.4 Mangrove and Terrestrial Organic Matter Dominate from 0 to 1000 Cal Yrs BP (Group 1)

From 0 to 1000 Cal yrs BP, organic matter provenance shifted from primarily freshwater phytoplankton debris (Group 2) to marine and terrestrial sources (Group 1). This period coincides with the expansion of pine on the Abaco landscape (at ~700 Cal yrs BP), and expansion of the wetland environment adjacent to the sinkhole based on the increase in *Conocarpus* (angiosperm, mangrove-associated shrub), other mangroves, and wetland plants (e.g., *Typha angustifolia*) in the last 1000 years. The core from the mangrove environment (BLWD-C6) was analyzed to investigate the impact of the mangrove environment on sinkhole sedimentation. The basal radiocarbon date in BLWD-C6 suggests that the wetland environment adjacent to Blackwood Sinkhole became established at least 1300 years ago. However, the,pollen record suggests abundant *Conocarpus* several centuries later by ~700 Cal yrs BP (Fig. 5). Based on just spatial sedimentation patterns, installation of the wetland environment likely helped to promote increased sedimentation towards the sinkhole center, as evidenced by the onset of significant sedimentation at BLWD-C3 after 1700 Cal yrs BP.

The statistical analysis and cross plots indicate that the organic matter of Group 1 (BLWD-C2, BLWD-C3) is most similar to the organic matter in the core extracted from the adjacent wetland (BLWD-C6). Within BLWD-C6, the average $\delta^{13}C_{org}$ value is $-26.9‰ \pm -0.5$ and $\delta^{15}N_{org}$ is $3.3‰ \pm 1.6$, but there is a notable ~1‰ change in $\delta^{13}C_{org}$

and a ~5‰ increase in $\delta^{15}N_{org}$ values downcore (Fig. 6). This enrichment in $\delta^{15}N_{org}$ values may be related to the preferential preservation of OM with a heavier $\delta^{15}N_{org}$ (Gonneea et al., 2004), or enhanced diagenesis of the organic matter in the oxic wetland environment altering its geochemical signature though time. The $\delta^{13}C_{org}$ and $\delta^{15}N_{org}$ values and C:N ratio signatures fall within accepted literature values for other mangrove species abundant in such marginal marine environments (including those fringed with *Rhizophora*, which is abundant within the Caribbean) (Gonneea et al., 2004; Larsen et al., 2012). Additional compound-specific lipids (e.g., taraxerol: (Versteegh et al., 2004)) could further elucidate the timing of increased mangrove organic matter flux to the sinkhole environment. Most importantly, the fresh organic matter from the coretop of BLWD-C6 did indeed have $\delta^{13}C_{org}$ and $\delta^{15}N_{org}$ values (~27‰ and 1.5‰) that are almost identical to mean values of $\delta^{13}C_{org}$ and $\delta^{15}N_{org}$ within group 1 of BLWD-C2 and BLWD-C3 (Table 2). This indicates the importance of the adjacent wetland for supplying OM to the sinkhole basin.

However, the consistent Λ8 values (Table 4, Figure 11) also indicate that the sinkhole is recording terrestrial changes from the surrounding landscape from 1000 years ago until present. A lower Syringyl/Vanillyl (S/V) LOP ratio is indicative of increased gymnosperms on the landscape (Table 4, Figure 11) (Hedges and Mann, 1979), which include plants such as pines. As previously discussed, pine trees (*Pinus*, gymnosperm) rapidly expand on the Abaco landscape at ~700 Cal yrs BP (Slayton, 2010, van Hengstum et al, 2016). These results indicate that although the adjacent wetland is contributing significant quantities of organic matter to Blackwood Sinkhole

through time, organic matter is also being supplied from the adjacent terrestrial landscape.

6.5 Potential Forcing of Organic Matter Changes

It is generally thought that meridional displacements of the Intertropical Convergence Zone (ITCZ) have significantly impacted the amount of Caribbean precipitation over millennial timescales (Hodell et al., 1991; Haug et al., 2001; Schneider et al., 2014). However, modern Caribbean precipitation is complex and variable over smaller geographic areas and impacted by multiple factors such as local atmospheric subsidence and divergence, or El Nino/Southern Oscillation (Gamble and Curtis, 2008; Jury et al., 2007). Potential changes in regional hydroclimate on centennial or millennial timescales are important to consider because changing rainfall can impact both groundwater (i.e., aquatic) and terrestrial ecosystems. The primary changes in landscape ecology that occurred from 1000 Cal yrs BP to present (i.e., from tropical hardwoods and palms to an oscillation between pine and *Conocarpus* dominance) is the most significant change in landscape ecology during the late Holocene on Abaco Island (Slayton, 2010, van Hengstum et al., 2016), and it is thought that this shift is in part caused by rainfall changes from related to a southern displacement of the ITCZ (van Hengstum et al. 2016). On nearby Andros Island, the increase in *Pinus* in the last 700 years has been interpreted as related to arrival of Lucayan natives on the island (Kjellmark, 1996), and a short-lived coastal wetland in Abaco dated to ~900 Cal yrs BP perhaps indicates increased rainfall or simply the autogenic re-organization of coastal environments (Steadman et al., 2014). Conversely, sedimentary and microfossil

evidence from a lagoon in northern Cuba suggests a regional drying trend at 1000 Cal yrs BP (Gregory et al., 2015), but an oxygen isotopic record from a speleothem in Cuba indicates increased rainfall at 1000 Cal yrs BP (Fensterer et al., 2013). These conflicting narratives of regional precipitation timed with critical landscape changes in the northern Caribbean emphasize the need for independent proxies of environmental and precipitation change to assess regional Caribbean responses late Holocene climate changes.

The geochemical results from the organic matter preserved in Blackwood Sinkhole suggest that a different hydroclimate conditions likely existed in Abaco Island from ~1500 to ~1000 Cal yrs BP (Group 2) than ~1000 Cal yrs BP to present (Group 1). Holocene sea-level rise and flooding of the epikarst surface likely did expand potential habitat availability for wetlands in Abaco Island over the late Holocene and enhance the flux of sediment to the sinkhole (Collins et al., 2015), but the amount of sea-level rise over the last 1000 years is most likely less than 50 cm (Milne and Peros, 2013; Steadman et al., 2014) to perhaps 1 m (Kovacs et al., 2013). Yet, there has been considerable expansion of wetlands in the last 1300 years adjacent to the sinkhole, with a suitable regional precipitation/evaporation ratio to supports these wetland environments. It remains challenging to disentangle the effects of climate forced precipitation and the effects of sea-level flooding the epikarst surface installing the wetland environment.The organic geochemical proxies measured within this thesis serve as indirect proxies for precipitation and still leave much still to be learned regarding late Holocene precipitation patterns in the Northern Bahamas.

7. CONCLUSIONS

Geochemical trends (from $\delta^{13}C_{org}$, $\delta^{15}N_{org}$, and C:N ratio proxies) in sediment cores from a sinkhole on Abaco Island, The Bahamas, likely reflect broader environmental change on the surrounding landscape and within the sinkhole itself during the last 3000 years. Quantification of LOP supports that there was consistent terrestrial input into Blackwood Sinkhole throughout the late Holocene, Variation in the geochemical signatures identifies three different intervals of time that are dominated by at least three different OM sources.

From 1500 to 3000 Cal yrs BP (Group 3), terrestrially-derived plants dominate OM source contributions to the sedimentary record. C:N values are highest within this interval, and C:N, $\delta^{13}C_{org}$, $\delta^{15}N_{org}$ signatures are consistent with literature values for terrestrial plants. This interval is well represented within BLWD-C2, which is on the periphery of the sinkhole basin, which is a location likely to record a strong terrestrial signal via input from the adjacent landscape. OM source contributions from 1000 to 1500 Cal yrs BP (Group 2) are dominated by freshwater phytoplankton, which is distinguished by enriched $\delta^{15}N_{org}$ values, and depleted $\delta^{13}C_{org}$. The C/V ratio increases during this time, indicative of soft tissue deposition, likely due to the *Lemna* recorded previously in the palynological record. From 0-1000 Cal yrs BP (Group 1), OM measured within Blackwood Sinkhole is almost identical to $\delta^{13}C_{org}$ and $\delta^{15}N_{org}$ values from the coretop, suggesting that the dominant OM contributions are coming from a marginal marine (adjacent mangrove) source. However, consistent LOP deposition, and a decrease in mean S/V ratio during this interval supports that this interval is

additionally recording a change in gymnosperm input to the OM. The palynological record complements the geochemical signatures, as a dominance in *Pinus* emerges at 1000 Cal yrs BP. Changes in $\delta^{13}C_{org}$, $\delta^{15}N_{org}$, and C:N ratio, relative to OM source contributions, serve as indirect proxies for larger scale landscape change within the Abaco region. This research supports the use of geochemical markers preserved the bulk organic matter deposited in karst basins to document regional landscape change, perhaps related to larger climatic and sea-level forcing.

REFERENCES

Bianchi, T. S., Mitra, S., M, & McKee, B. (2002). Sources of terrestrially-derived organic carbon in lower Mississippi River and Louisiana shelf sediments: implications for differential sedimentation and transport at the coastal margin. *Marine Chemistry, 77*, 211-223.

Brandenberger, J. M., Louchouarn, P., & Crecelius, E. A. (2011). Natural and Post-Urbanization Signatures of Hypoxia in Two Basins of Puget Sound: Historical Reconstruction of Redox Sensitive Metals and Organic Matter Inputs. *Aquatic Geochemistry, 17*(4-5), 645-670. doi:10.1007/s10498-011-9129-0

Carew, J. L., & Mylroie, J. E. (1997). Geology of the Bahamas. In L. Vacher & T. Quinn (Eds.), *Geology and Hydrogeology of Carbonate Islands, Developments in Sedimentology* (pp. 91-139). Amersterdam: Elsevier Science Publishers

Chiang, J. C. H. K., Yochanan; Giannini, Alessandra. (2002). Deconstructing Atlantic Intertropical Convergence Zone variability: Influence of the local cross-equatorial sea surface temperature gradient and remote forcing from the easter equatorial Pacific. *Journal of Geophysical Research, 107*, 3-2-3-19.

Collins, S. V., Reinhardt, E. G., Werner, C. L., Le Maillot, C., Devos, F., & Rissolo, D. (2015). Late Holocene mangrove development and onset of sedimentation in the Yax Chen cave system (Ox Bel Ha) Yucatan, Mexico: Implications for using cave sediments as a sea-level indicator. *Palaeogeography, Palaeoclimatology, Palaeoecology, 438*, 124-134.

Dittmar, T., Lara, R. J., & Kattner, G. (2001). River or mangrove? Tracing major organic matter sources in tropical Brazilian coastal waters. *Marine Chemistry, 73*, 253-271.

Duck, R. W. (1986). Bottom sediments of Loch Tummel, Scotland. *Sedimentary Geology, 47*, 293-315.

Farella, N., Lucotte, M., Louchouarn, P., & Roulet, M. (2001). Deforestation modifying terrestrial organic transport in the Rio Tapajos, Brazilian Amazon. *Organic Geochemistry, 32*(12), 1443-1458. doi:Doi 10.1016/S0146-6380(01)00103-6

Feng, X., Gustafsson, Ö., Holmes, R. M., Vonk, J. E., van Dongen, B. E., Semiletov, I. P., . . . Eglinton, T. I. (2015). Multi-molecular tracers of terrestrial carbon transfer across the pan-Arctic – Part 1: Comparison of hydrolysable components with plant wax lipids and lignin phenols. *Biogeosciences Discussions, 12*(6), 4721-4767. doi:10.5194/bgd-12-4721-2015

Fensterer, C., Scholz, D., Hoffmann, D., Spotl, C., Pajon, J. M., & Mangini, A. (2012). Cuban stalagmite suggests relationship between Caribbean precipitation and the Atlantic Multidecadal Oscillation during the past 1.3 ka. *The Holocene, 22*(12), 1405-1412. doi:10.1177/0959683612449759

Fensterer, C., Scholz, D., Hoffmann, D. L., Spötl, C., Schröder-Ritzrau, A., Horn, C., . . . Mangini, A. (2013). Millennial-scale climate variability during the last 12.5ka recorded in a Caribbean speleothem. *Earth and Planetary Science Letters, 361*, 143-151. doi:10.1016/j.epsl.2012.11.019

Filley, T. R., Freeman, K. H., Bianchi, T. S., Baskaran, M., Colarusso, L. A., & Hatcher, P. G. (2001). An isotopic biogeochemical assessment of shifts in organic matter input to Holocene sediments from Mud Lake, Florida. *Organic Geochemistry, 32*, 1153-1167.

Fogel, M. L., & Cifuentes, L. A. (1993). Isotope Fractionation during Primary Production. In M. H. Engel & S. A. Macko (Eds.), *Organic Geochemistry, Principles and Applications* (pp. 73-94). New York, USA: Springer Science+Business.

Gamble, D. W., & Curtis, S. (2008). Caribbean precipitation: review, model and prospect. *Progress in Physical Geography, 32*(3), 265-276. doi:10.1177/0309133308096027

Gieskes, W. W. C., Kraay, G. W., & Baars, M. A. (1979). Current 14C methods for measuring primary production: gross underestimates in oceanic waters. *Netherlands Journal of Sea Research, 13*(1), 58-78.

Goni, M. (1997). Record of Terrestrial Organic Matter Composition in Amazon Fan Sediments. *Proceedings of the Ocean Drilling Program, Scientific Results, 155*, 519-530.

Goni, M., & Thomas, K. A. (2000). Source and Transformations of Organic Matter in Surface Soils and Sediments from a Tidal Estuary (North Inlet, South Caroline, USA). *Estuaries, 23*(4), 548-564.

Gonneea, M. E., Paytan, A., & Herrera-Silveira, J. A. (2004). Tracing organic matter sources and carbon burial in mangrove sediments over the past 160 years.

Estuarine, Coastal and Shelf Science, 61(2), 211-227. doi:10.1016/j.ecss.2004.04.015

Gouveia, S. E. M., Pessenda, L. C. R., Aravena, R., Boulet, R., Scheel-Ybert, R., Bendassoli, J. A., . . . Freitas, H. A. (2002). Carbon isotopes in charcoal and soils in studies of paleovegetation and climate changes during the late Pleistocene and the Holocene in the southeast and centerwest regions of Brazil. *Global and Planetary Change, 33*, 95-106.

Gregory, B. R. B., Peros, M., Reinhardt, E. G., & Donnelly, J. P. (2015). Middle-late Holocene Caribbean aridity inferred from foraminifera and elemental data in sediment cores from two Cuban lagoons. *Palaeogeography, Palaeoclimatology, Palaeoecology, 426*, 229-241.

Hammer, O., Harper, D. A. T., & Ryan, P. D. (2001). PAST: Paleontological statistics software package for education and data analysis. *Paleontologia Electronica, 4*(1).

Haug, G. H., Gunther, D., Peterson, L. C., Sigman, D., Hughen, K. A., & Aeschlimann, B. (2003). Climate and the Collapse of Maya Civilization. *Science*(299), 1731-1735.

Haug, G. H., Hughen, K. A., Sigman, D. M., Peterson, L. C., & Rohhl, U. (2001). Southward migration of the intertropical convergence zone through the Holocene. *Science, 293*, 1304-1308.

Hedges, J. I., & Ertel, J. R. (1982). Characterization of Lignin by Gas Capillary Chromatography of Cupric Oxide Oxidation Products. *Analytical Chemistry, 54*, 174-178.

Hedges, J. I., Keil, R. G., & Benner, R. (1997). What happens to terrestrial organic matter in the ocean? *Organic Geochemistry, 27*(5/6), 195-212.

Hedges, J. I., & Mann, D. C. (1979). The characterization of plant tissues by their lignin oxidation products. *Geochemica et. Cosmochemica et Acta, 43*, 1803-1807.

Hedges, J. I., & Parker, P. (1976). Land-derived organic matter in surface sediments from the Gulf of Mexico. *Geochemica et. Cosmochemica Acta, 40*, 1019-1029.

Hodell, D. A., Curtis, J. H., Jones, G. A., Higuera-Gundy, A., Brenner, M., Binford, M., & Dorsey, K. T. (1991). Reconstruction of Caribbean climate change over the past 10,500 years. *Nature, 352*, 790-793.

Houel, S., Louchouarn, P., & Lucotte, M. (2006). Translocation of soil organic matter following reservoir impoundment in boreal systems: Implications for in situ productivity. *Limnological Oceanography, 51*(3), 1497-1513.

Jury, M., Malmgren, B. A., & Winter, A. (2007). Subregional precipitation climate of the Caribbean and relationships with ENSO and NAO. *Journal of Geophysical Research, 112*(D16), 1-10. doi:10.1029/2006jd007541

Keegan, W. F. (1992). *The people who discovered Columbus: the prehistory of the Bahamas*. Gainesville, Florida: University Press of Florida.

Keeley, J. E., & Sandquist, D. R. (1992). Carbon: freshwater plants. *Plant, Cell and Environment, 15*, 1021-1035.

Kjellmark, E. (1996). Late Holocene climate change and human disturbance on Andros Island, Bahamas. *Journal of Paleolimnology, 15*, 133-145.

Kovacs, S. E., van Hengstum, P. J., Reinhardt, E. G., Donnelly, J. P., & Albury, N. A. (2013). Late Holocene sedimentation and hydrologic development in a shallow coastal sinkhole on Great Abaco Island, The Bahamas. *Quaternary International, 317*, 118-132. doi:10.1016/j.quaint.2013.09.032

Ladd, S. N., & Sachs, J. P. (2015). Hydrogen isotope response to changing salinity and rainfall in Australian mangroves. *Plant Cell Environ, 38*(12), 2674-2687. doi:10.1111/pce.12579

Lamb, A. L., Wilson, G. P., & Leng, M. J. (2006). A review of coastal palaeoclimate and relative sea-level reconstructions using δ13C and C/N ratios in organic material. *Earth-Science Reviews, 75*(1-4), 29-57. doi:10.1016/j.earscirev.2005.10.003

Lane, C. S., Horn, S. P., & Kerr, M. T. (2014). Beyond the Mayan Lowlands: impacts of the Terminal Classic Drought in the Caribbean Antilles. *Quaternary Science Reviews, 86*, 89-98. doi:10.1016/j.quascirev.2013.12.017

Larsen, R. K., Schantz, M. M., & Wise, S. A. (2006). Determination of Levoglucosan in Particulate Matter Reference Materials. *Aerosol Science and Technology, 40*(10), 781-787. doi:10.1080/02786820600596909

Lee-Thorp, J. A., Holmgren, K., Lauritzen, S. E., Linge, H., Moberg, A., Partridge, T. C., . . . Tyson, P. D. (2001). Rapid climate shifts in the southern African interior

throughout the mid to late Holocene. *Geophysical Research Letters, 28*(23), 4507-4510.

Louchouarn, P., Amon, R. M. W., Duan, S., Pondell, C., Seward, S. M., & White, N. (2010). Analysis of lignin-derived phenols in standard reference materials and ocean dissolved organic matter by gas chromatography/tandem mass spectrometry. *Marine Chemistry, 118*(1-2), 85-97. doi:10.1016/j.marchem.2009.11.003

Louchouarn, P., Lucotte, M., Canuel, R., Gagne, J. P., & Richard, L.-F. (1997). Sources and early diagenesis of lignin and bulk organic matter in the sediments of the Lower St. Lawrence Estuary and the Saguenay Fjord. *Marine Chemistry, 58*, 3-26.

Louchouarn, P., Lucotte, M., & Farella, N. (1991). Historical and geographical variations of sources and transport of terrigenous organic matter within a large-scale coastal environment. *Organic Geochemistry, 30*, 675-699.

Louchouarn, P., Lucotte, M., & Farella, N. (1999). Historical and geographical variations of sources and transport of terrigenous organic matter within a large-scale coastal environment. *Organic Geochemistry, 30*, 675-699.

Louchouarn, P., Naehr, T. H., Silliman, J., & Houel, S. (2006). Elemental, Stable Isotopic (13C) and molecular signatures of organic matter in Late Plesitocene-Holocene sediments from the Peruvian margin (ODP Site 1229). *Proceedings of the Ocean Drilling Program, Scientific Results, 201*, 1-21.

Makou, M. C., Eglinton, T. I., Oppo, D. W., & Hughen, K. A. (2010). Postglacial changes in El Nino and La Nina behavior. *Geology, 38*(1), 43-46. doi:10.1130/g30366.1

Martin, J. B., Gulley, J., & Spellman, P. (2012). Tidal pumping of water between Bahamian blue holes, aquifers, and the ocean. *Journal of Hydrology, 416-417*, 28-38. doi:10.1016/j.jhydrol.2011.11.033

Meyers, P. A. (1994). Preservation of elemental and isotopic source identification of sedimentary organic matter. *Chemical Geology, 114*, 289-302.

Meyers, P. A., & Lallier-Verges, E. (1999). Lacustrine sedimentary organic matter records of Late Quaternary paleoclimates. *Journal of Paleolimnology, 21*, 345-372.

Milne, G. A., & Peros, M. (2013). Data-model comparison of Holocene sea-level change in the circum-Caribbean region. *Global and Planetary Change, 107*, 119-131.

Mylroie, J. E., & Vacher, H. (1999). *A conceptual view of carbonate island karst.* Paper presented at the Karst Modeling Symposium, Charlottesville Virginia.

Mylroie, J. E. C., James L.; Moore, Audra I. . (1995). Blue Holes: Definition and Genesis. *Carbonates and Evaporites, 10*(2), 225-233.

Natelhoffer, K. J., & Fry, B. (1988). Controls on natural nitrogen-15 and carbon-13 abundances in forest soil organic matter. *Soil Science Society of America Journal, 52*(6), 1633-1640.

O'Leary, M. (1981). Carbon isotope fractionation in plants. *Phytochemistry, 20*(4), 553-567.

O'Leary, M. H. (1988). Carbon isotopes in photosynthesis. *BioScience, 38*(5), 328-336.

Ogrinc, N., Fontolan, G., Faganeli, J., & Covelli, S. (2005). Carbon and nitrogen isotope compositions of organic matter in coastal marine sediments (the Gulf of Trieste, N Adriatic Sea): indicators of sources and preservation. *Marine Chemistry, 95*(3-4), 163-181. doi:10.1016/j.marchem.2004.09.003

Park Boush, L. E., Myrbo, A., & Michelson, A. (2014). A qualitative and quantitative model for climate-drive lake formation on carbonate platforms based on examples from the Bahamian archipelago. *Carbonates and Evaporites, 29*, 409-418. doi:10.1007/s13146-014-0221-6

Peters, K. E., Sweeney, R. E., & Kaplan, I. R. (1978). Correlation of carbon and nitrogen stable isotope ratios in sedimentary organic matter. *Association for the Sciences of LImnology and Oceanography, 23*(4), 598-604.

Phillips, D. L., & Koch, P. L. (2002). Incorporating concentration dependence in stable isotope mixing models. *Oecologia, 130*(1), 114-125. doi:10.1007/s004420100786

Phillips, D. L., Newsome, S. D., & Gregg, J. W. (2005). Combining sources in stable isotope mixing models: alternative methods. *Oecologia, 144*(4), 520-527. doi:10.1007/s00442-004-1816-8

Prahl, F. G., Bennett, J. T., & Carpenter, R. (1980). The early diagenesis of aliphatic hydrocarbons and organic matter in sedimentary particulates from Dabob Bay, Washington. *Geochimica et Cosmochimica Acta, 44*, 1967-1976.

Sachse, D., Billault, I., Bowen, G. J., Chikaraishi, Y., Dawson, T. E., Feakins, S. J., . . . Kahmen, A. (2012). Molecular Paleohydrology: Interpreting the Hydrogen-Isotopic Composition of Lipid Biomarkers from Photosynthesizing Organisms. *Annual Review of Earth and Planetary Sciences, 40*(1), 221-249. doi:10.1146/annurev-earth-042711-105535

Schneider, T., Bischoff, T., & Haug, G. H. (2014). Migrations and dynamics of the intertropical convergence zone. *Nature, 513*(7516), 45-53. doi:10.1038/nature13636

Slayton, I. A. (2010). *A vegetation history from Emerald Pond, Great Abaco Island, the Bahamas, based on pollen analysis.* (Master of Science), University of Tennessee-Knoxville, University of Tennessee-Knoxville.

Steadman, D. W., Albury, N. A., Maillis, P., Mead, J. I., Slapcinsky, J., Krysko, K. L., . . . Franklin, J. (2014). Late-Holocene faunal and landscape change in the Bahamas. *The Holocene, 24*(2), 220-230.

Steadman, D. W., Franz, R., Morgan, G., Albury, N. A., Kakuk, B., Broad, K., . . . Dilcher, D. L. (2007). Exceptionally well preserved late Quaternary plant and vertebrate fossils from a blue hole on Abaco, The Bahamas. *Proceedings of the National Academy of the Sciences, 104*(50), 19897-19902.

Talbot, M. R., & Laerdal, T. (2000). The Late Pleistocene- Holocene palaeolimnology of Lake Victoria, East Africa, based upon elemental and isotopic analyses of sedimentary organic matter. *Journal of Paleolimnology, 23*, 141-164.

van Hengstum, P. J., Donnelly, J. P., Fall, P. L., Toomey, M. R., Albury, N. A., & Kakuk, B. (2016). The intertropical convergence zone modulates intense hurricane strikes on the western North Atlantic margin. *Scientific Reports, 6*, 1-10. doi:10.1038/srep21728

van Hengstum, P. J., Reinhardt, E. G., Beddows, P. A., & Gabriel, J. J. (2010). Linkages between Holocene paleoclimate and paleohydrogeology preserved in a Yucatan underwater cave. *Quaternary Science Reviews, 29*(19-20), 2788-2798. doi:10.1016/j.quascirev.2010.06.034

van Hengstum, P. J., Scott, D. B., Gröcke, D. R., & Charette, M. A. (2011). Sea level controls sedimentation and environments in coastal caves and sinkholes. *Marine Geology, 286*(1-4), 35-50. doi:10.1016/j.margeo.2011.05.004

Versteegh, G. J. M., Schefuß, E., Dupont, L., Marret, F., Sinninghe Damsté, J. S., & Jansen, J. H. F. (2004). Taraxerol and Rhizophora pollen as proxies for tracking past mangrove ecosystems. *Geochimica et Cosmochimica Acta, 68*(3), 411-422. doi:10.1016/s0016-7037(03)00456-3

Visser, K., Thunell, R., & Goni, M. (2004). Glacial–interglacial organic carbon record from the Makassar Strait, Indonesia: implications for regional changes in continental vegetation. *Quaternary Science Reviews, 23*(1-2), 17-27. doi:10.1016/j.quascirev.2003.07.001

Waliser, D. E., & Gautier, C. (1993). A satellite-derived climatology of the ITCZ. *Journal of Climate, 6*, 2162-2174.

Wilson, G. P., Lamb, A. L., Leng, M. J., Gonzalez, S., & Huddart, D. (2005). δ13C and C/N as potential coastal palaeoenvironmental indicators in the Mersey Estuary, UK. *Quaternary Science Reviews, 24*(18-19), 2015-2029. doi:10.1016/j.quascirev.2004.11.014

Zimmerman, A. R., & Canuel, E. A. (2002). Sediment geochemical records of eutrophication in the mesohaline Cheaspeake Bay. *Limnological Oceanography, 47*(4), 1084-1093.